

## Exploring the Synthetic Potential of Dihydroxyacetone- Aldolases from Acidophilic Organisms

Léo Paulat,<sup>[a]</sup> Cédric Gastaldi,<sup>[a]</sup> Lionel Nauton,<sup>[a]</sup> Mariline Theveniot,<sup>[a]</sup> Muriel Joly,<sup>[a]</sup> Jean-Louis Petit,<sup>[b]</sup> Véronique de Berardinis,<sup>[b]</sup> Virgil Hélaine\*<sup>[a]</sup> and Christine Guérard-Hélaine\*<sup>[a]</sup>

[a] Université Clermont Auvergne, Clermont Auvergne INP, CNRS, Institut de Chimie de Clermont-Ferrand, 63000 Clermont-Ferrand, France ; e-mail: christine.helaine@uca.fr

[b] Génomique Métabolique, Génoscope, Institut François Jacob, CEA, CNRS, Univ Evry, Université Paris-Saclay, Evry-Courcouronnes, 91057 Evry, France.

Material .....	2
Methods .....	3
1. Database exploration .....	3
2. Purification and biochemical characterization of the enzymes.....	4
2.1. Cloning, expression and purification of the recombinant enzymes .....	4
2.2. Activity assays.....	6
2.3. Optimum pH determination .....	8
2.4. Enzyme thermostability.....	9
2.5. Kinetic constants .....	13
2.6. Isotopic exchange measurements on nucleophiles by <sup>1</sup> H NMR .....	14
3. Molecular modelling.....	22
3.1. Construction of the structures .....	22
3.2. Docking experiments .....	24
4. Electrophiles study .....	26
5. Syntheses.....	26
5.1. D-threose from glycolaldehyde.....	26
5.2. 2-deoxy-D-ribose-5-phosphate from acetaldehyde + D-glyceraldehyde-3-phosphate.....	29
5.3. (3S,4S) 5-chloro-3,4-dihydroxypentan-2-one from HA + chloroacetaldehyde .....	30
5.4. (3S,4S) 3,4-dihydroxypentanal from acetaldehyde + L-lactaldehyde .....	32
References.....	35



## Material

D-fructose-6-phosphate dipotassium salt,  $\alpha$ -glycerophosphate dehydrogenase, D-arabinose-5-phosphate, alcohol dehydrogenase from *Saccharomyces cerevisiae*, Trizma hydrochloride, sodium phosphate monobasic dihydrate, hydroxyacetone, 1,3-dihydroxyacetone dimer, glycolaldehyde dimer, 3,3-diethoxy-1-propanol, acetaldehyde, 5-hydroxypentan-2-one and chloroacetaldehyde 55% in water were purchased from Sigma-Aldrich whereas  $\beta$ -nicotinamide adenine dinucleotide reduced disodium salt hydrate (NADH) and glycylglycine were purchased from Alfa Aesar. D-arabinose was purchased from Fluka and acetone from Carlo Erba. The Coomassie protein assay reagent, used for Bradford tests, was purchased from Thermo Scientific. Protein desalting columns were purchased from GE Healthcare and Ni-NTA-agarose was purchased from Qiagen. VWR centrifugal filters were purchased from VWR North America Cat. Glycerol dehydrogenase was obtained as described by A.K. Samland.<sup>1</sup>

Nuclear magnetic resonance (NMR) spectra were recorded using D<sub>2</sub>O as solvent on a Bruker AC-400 spectrometer, operating at 400 MHz for <sup>1</sup>H and 100 MHz for <sup>13</sup>C. Chemical shifts ( $\delta$ ) are reported in ppm relative to TMS signal. Coupling constant values ( $J$ ) are given in Hertz. Electrospray ionization mass spectra (ESI-MS) were recorded on a micro Orbitrap Q-Exactive (70000 V) and high-resolution mass spectra (HR-MS) were recorded on the same instrument with an internal lock mass (H<sub>3</sub>PO<sub>4</sub>) and an external lock mass (Leu-enkephalin).

# Methods

## 1. Database exploration

Uniprot ID	Organism
P78055	<i>Escherichia coli</i> (strain K12)
P32669	<i>Escherichia coli</i> (strain K12)
A0A0E4G3U3	<i>Listeria monocytogenes</i> serovar 1/2a (strain ATCC BAA-679 / EGD-e)
A0A0D6J3Z8	<i>Streptococcus pneumoniae</i>
Q8DVJ4	<i>Streptococcus mutans</i> serotype c (strain ATCC 700610 / UA159)
A0A0D6H018	<i>Streptococcus pyogenes</i>
A0A0E4C363	<i>Streptococcus gordonii</i>
Q8E738	<i>Streptococcus agalactiae</i> serotype III (strain NEM316)
A0A0E4C393	<i>Streptococcus suis</i>

Table S1. Reference set composed of already identified FSA

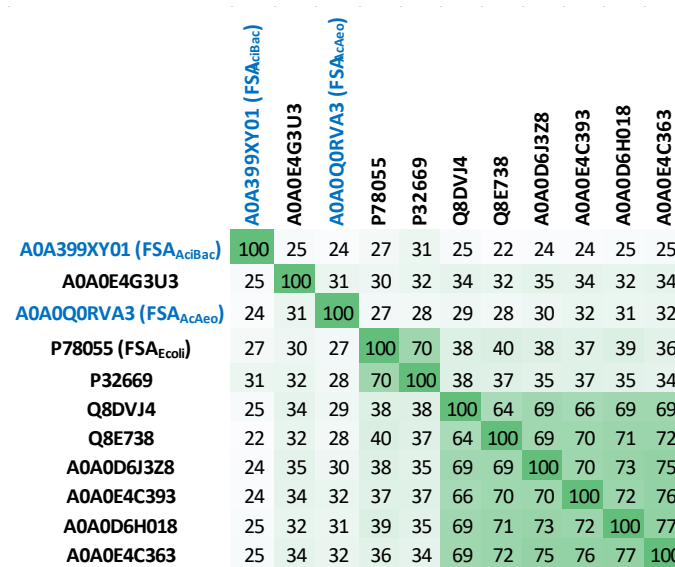
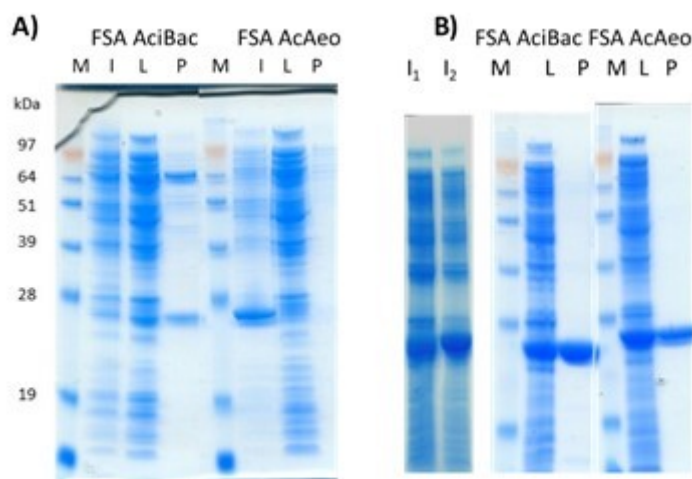


Figure S1. Matrix of identity percentage between FSA from the reference set and the two FSA candidates from acidophilic bacteria (written in blue)





**Figure S3 :** SDS-gels of A) N-terminally tagged or B) C-terminally tagged studied proteins throughout the various stages of production and purification of the 2 enzymes. I: induction culture (I1: related to FSA AciBac, I2: to FSA AcAeo), L: clear lysate (obtained after sonication and centrifugation), P: purified lysate (obtained after purification by IMAC technique) and M: Molecular mass marker.

	Primer-5Prim	Primer-3Prim	optimized sequence
FSA AciBac	AAAGAA GGAGAT AGGATC ATGGCC ATCTTTC TTGACT CAGCC	GTGTAA TGGATA GTGATC TTAATG GTGATG GTGATG ATGCTT TGAAGC ACCGGA TTGGG	ATGGCCATCTTTCTTGACTCAGCCGATGTTGCGGATGCGGAATGTGCACGTCAGCTGGGTTTCGT GGCTGGTGTACGACCAACCCCAAACCTGCTGGCGGGAGCGAATCCTTTGGCACGTATTCCGGAAC TGCTGGATGCCATTCTGACGTTCCAGTATGTTGTCAATTAACAGAGTTGGATGATGCGAAAGCG TTTCTCGCACAAGGAGAGCGCTGCACGCCTTAGACCCAGAACCGTGGTTATTAAGGTTCCGAC GCGCACCGAAACCCCTTAACCTTAGCGTGCCAGCTGATTGAACGCGGTATCCCATGTGCCATGACCA CTATTTTCTCTCCGGAGCAGGCATTAATCGCAGGCGAAATTGGCGCGCCTGGGTTATCCGTAC GTGGATCGTACTACGCGCTCGGCGGTGATGGCCTGGAATGGTATCTGAAATGCGCCGATTTT GGACGCCATTGGTGCAGCAGCGTGTGATGGCGGGTCCATTAAGGCGCTGCCGGTGTGGCAC GCATCGTGAAGCGGGTGCACATGACGTAACCGCCTCGTGGATGTTGTGAAAGAATTAGGTAAC CACGAATGGAGCGAGCGAGCATCGCTGATTTTCGCGGAAGCGCCAATCCGGTGCTCAAAGTAA
FSA AcAeo	AAAGAA GGAGAT AGGATC ATGAAG ATTTTCC TTGACT CGGCG	GTGTAA TGGATA GTGATC TTAATG GTGATG GTGATG ATGCTG ATTGAA GAACGT CTTC	ATGAAGATTTTCTTGACTCGCGCAACATCGACGAGATTAACAACATCGCGCTATGGTATCTTGG ACGGTATCACTACTAACCCAAGCATTCTGTCCAAGAGTTGACGATAACAACGACACGGCAGGCA TTATCAATAACATCATTAAAGCAGTAAACGGAGAAGTTCATATCAAGTCACGAGTGACGAGTATGA TACGATCTGAAGCAAGCAATGAAGATTCCTGCTCGGCTTGAACGTCATCGTCAAAATCCCGGTA ACCCAGAACGGTATGGCAGCCATGGCAGCCTTCGCTCGCGGGTATCAAGATCAATGCGACAAC ATTTTCAGCCATTACAAGCCCTGGCGGGCGGAAGAACAACGCGGAGTACAGCACCCTGACCTG AGTCCATTGACGACAGTGGGAATAGCAGCTACAAAGTATCCAGACCATCCGCACTATGTTCAACA ACTACAACATGAAGACTAAGATTATGGGTGCGGCCATCAAGAACCCGGTCCAATATTGAATGTG GCATGGCGGGCGTGGATGCAGTGACCGCTCCGTACGGGGTCTCAAAATAATGCTTGATCATCCCGA GACTCTTATGAACGTGAATCGCTTCATTAAGATTGGAACCTCATCCCGCAAATTCGAAGACGTTT TTCAATCAGTAA

**Table S2.** Primers and optimized sequences for FSA<sub>AcBac</sub> and FSA<sub>AcAeo</sub>

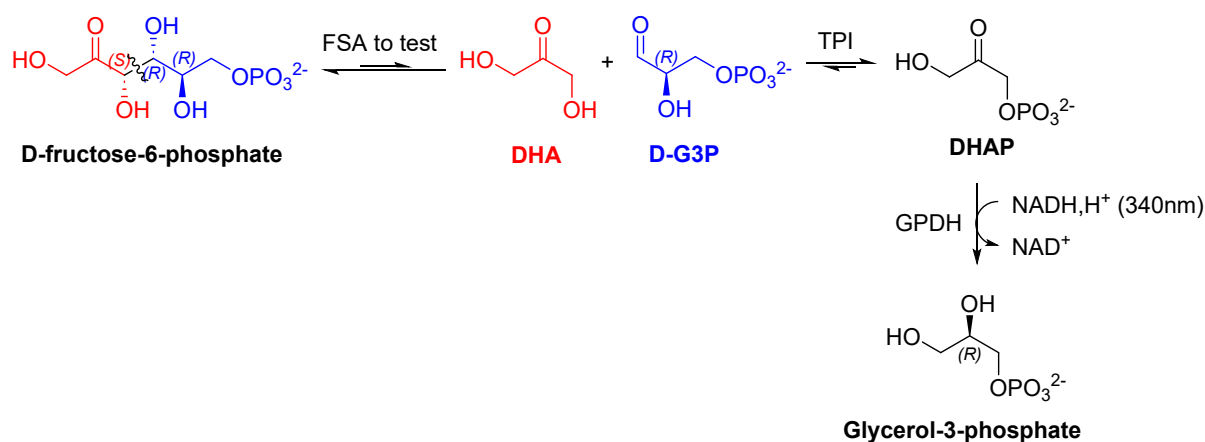
Protocol for 1 L culture: *E. coli* colonies (expression strain) containing the plasmids were cultured in 1 L of Luria-Bertani (LB) broth in the presence of a selection antibiotic (ampicillin) at 37°C with shaking. When the culture reached an OD<sub>600nm</sub> of 0.5, protein expression was induced with IPTG (0.5 mM) and the temperature was dropped to 30°C. The culture was incubated for a further period of 12 h. Cells were harvested by centrifugation, washed twice and resuspended in buffer A (50 mM NaH<sub>2</sub>PO<sub>4</sub>, 300 mM NaCl, pH 8.0). Cell

suspension was disrupted by sonication and the cell lysate was centrifuged at 10000 x g for 20 min. Clear supernatant was loaded onto a Ni<sup>2+</sup>-NTA-agarose column (Qiagen, h=3 cm; Ø=2.5 cm) pre-equilibrated with buffer A containing 10 mM of imidazole (buffer B). The column was washed with buffer B, and the retained proteins were eluted with the same buffer containing 500 mM of imidazole. Eluted fraction containing pure protein was dialyzed against water for desalting and imidazole removal before the lyophilization process. For FSA<sub>AcBac</sub> 373 mg of enzyme were obtained. For FSA<sub>AcAeo</sub> during the dialysis step, a 3M ammonium sulfate solution was added. The protein concentration was then determined by Bradford, resulting in 290 mg of enzyme obtained as a 29 mg/mL solution.

## 2.2. Activity assays

### Specific activity towards D-fructose-6-phosphate :

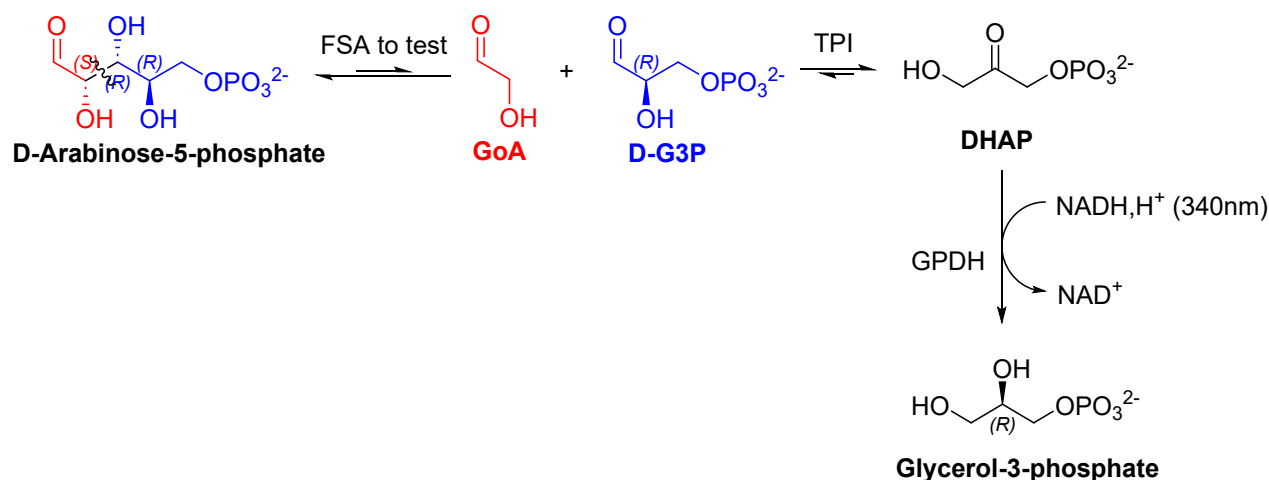
To a solution of D-fructose-6-phosphate (10 mM), DHA aldolase (96 µg of FSA<sub>AcBac</sub> or 47 µg of FSA<sub>AcAeo</sub>) in 50 mM glycyl-glycine buffer pH 7.5, was added at 25°C. NADH (0.5 mM), the auxiliary enzymes triose-phosphate isomerase (TPI) and glycerol-3-phosphate dehydrogenase (GPDH) (10 U and 1 U respectively) were added to isomerise D-glyceraldehyde-3-phosphate formed and reduce subsequent dihydroxyacetone phosphate (DHAP). The final volume was 1 mL. The reaction was monitored by spectrophotometry at 340 nm following the consumption of NADH. One mmol of NADH oxidized was equivalent to 1 mmol of D-fructose-6-phosphate cleaved. One unit (U) of DHA aldolase is defined as the amount of enzyme able to cleave 1 µmol of D-fructose-6-phosphate to afford D-glyceraldehyde-3-phosphate and dihydroxyacetone phosphate per minute. A specific activity of 11 mU/mg for FSA<sub>AcBac</sub> and 151 mU/mg for FSA<sub>AcAeo</sub> were found.



### Specific activity towards D-arabinose-5-phosphate:

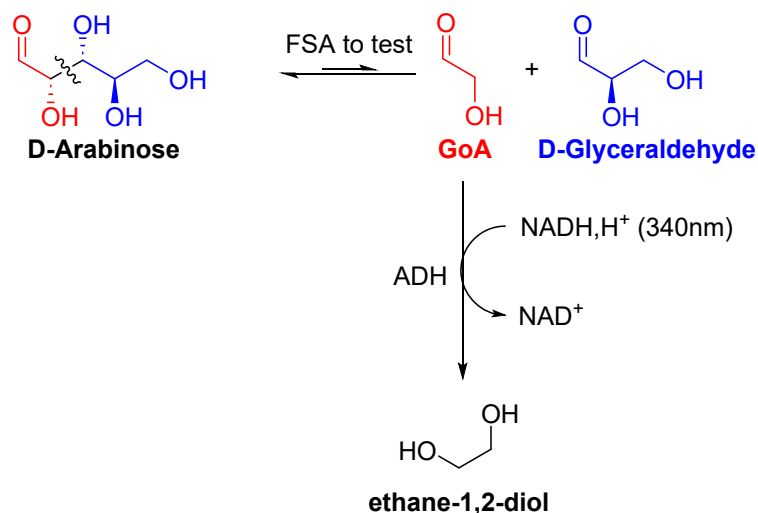
The spectrophotometric assays were recorded on a Safas UVMC2 (Safas, Monaco) using microcells high-precision cell quartz with 10 mm light path (Hellma Analytics,

Müllheim, Germany) in a volume of 100  $\mu\text{l}$ . To a solution of 5 mM D-arabinose-5-phosphate, 0.3 mM NADH in 50 mM glycyl-glycine buffer pH 7.5 with the auxiliary enzymes triose-phosphate isomerase and glycerol-3-phosphate dehydrogenase (TPI and GPDH: 10 U and 1 U respectively), DHA aldolase (0.25  $\mu\text{g}$  of FSA<sub>AcBac</sub> or 0.25  $\mu\text{g}$  of FSA<sub>AcAeo</sub>) was added at 25°C. The reaction was monitored at 340 nm following the consumption of NADH. One mmol of NADH oxidized was equivalent to 1 mmol of D-arabinose-5-phosphate cleaved. One unit (U) of DHA aldolase is defined as the amount of enzyme able to cleave 1  $\mu\text{mol}$  of D-arabinose-5-phosphate to afford D-glyceraldehyde-3-phosphate per minute. A specific activity of 3.7 U/mg for FSA<sub>AcBac</sub> and 0.03 U/mg for FSA<sub>AcAeo</sub> were found.



#### Specific activity towards D-arabinose :

To a solution of D-arabinose (300 mM) in 50 mM glycyl-glycine buffer pH 7.5, DHA aldolase (10  $\mu\text{g}$  of FSA<sub>AcBac</sub> or 5  $\mu\text{g}$  of FSA<sub>AcAeo</sub>) and NADH (0.5 mM) were added at 25°C. The auxiliary enzyme alcohol dehydrogenase 20  $\mu\text{L}$  (560 U) was added to reduce glycolaldehyde (GoA). The final volume was 1 mL. The reaction was monitored by spectrophotometry at 340 nm following the consumption of NADH. One mmol of NADH oxidized was equivalent to 1 mmol of D-arabinose cleaved. One unit (U) of DHA aldolase is defined as the amount of enzyme able to cleave 1  $\mu\text{mol}$  of D-arabinose to afford glycolaldehyde per minute. A specific activity of 640 mU/mg for FSA<sub>AcBac</sub> and 1 U/mg for FSA<sub>AcAeo</sub> were found.



### 2.3. Optimum pH determination

FSA optimum pH was calculated assaying its retroaldol activity at pH values between 6.0 and 9.0 in 50 mM of glycylglycine, Tris-HCl and phosphate buffer. Activities were determined by measuring the formation of D-glyceraldehyde-3-phosphate (D-G3P) from 5 mM of D-arabinose-5-phosphate, with 0,3 mM NADH and the auxiliary enzymes triose-phosphate isomerase and glycerol-3-phosphate dehydrogenase (10 U and 1 U respectively), for FSA<sub>AcBac</sub> (2.5 µg/ml). Concerning FSA<sub>AcAeo</sub>, formation of glycolaldehyde was followed from 25 mM of D-arabinose with 25 µg/ml FSA<sub>AcAeo</sub> for glycylglycine and Tris-HCl buffer or 50 µg/ml for phosphate buffer, with 0.4 mM NADH and the auxiliary enzyme alcohol dehydrogenase (371 U). The reaction was monitored at 340 nm following the consumption of NADH. Variations of  $A_{340\text{nm}}$  were proportional to formation of D-G3P for FSA<sub>AcBac</sub> or formation of glycolaldehyde for FSA<sub>AcAeo</sub> in reaction ( $\epsilon_{\text{NADH}} = 6220 \text{ cm}^{-1}\text{M}^{-1}$ ).



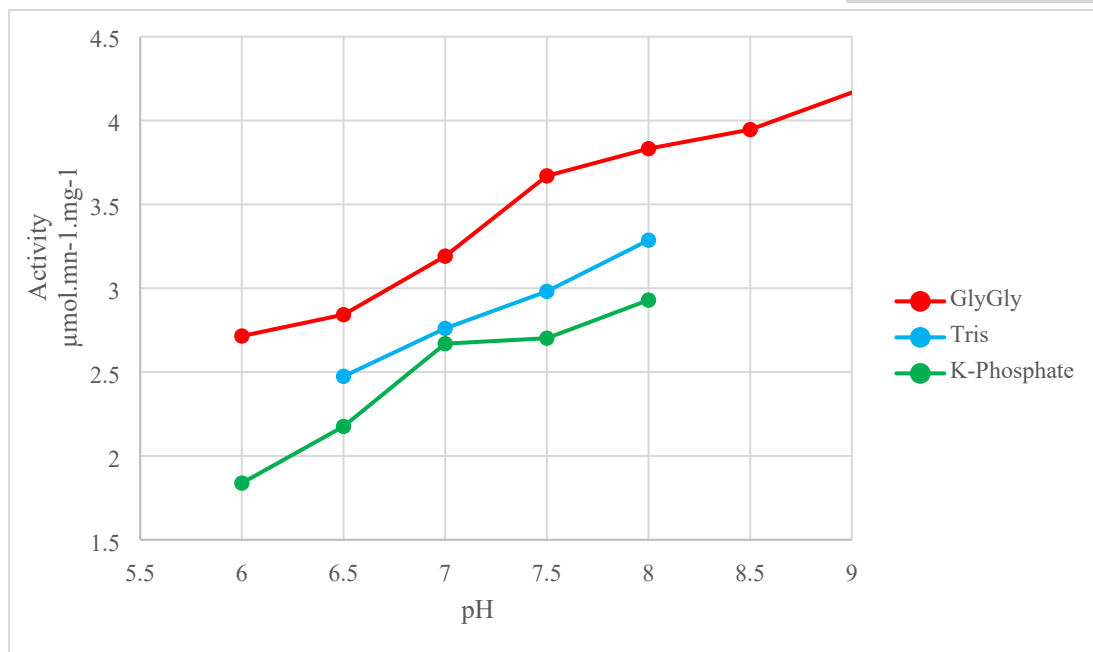


Figure S4 : pH study for FSA<sub>AciBac</sub>

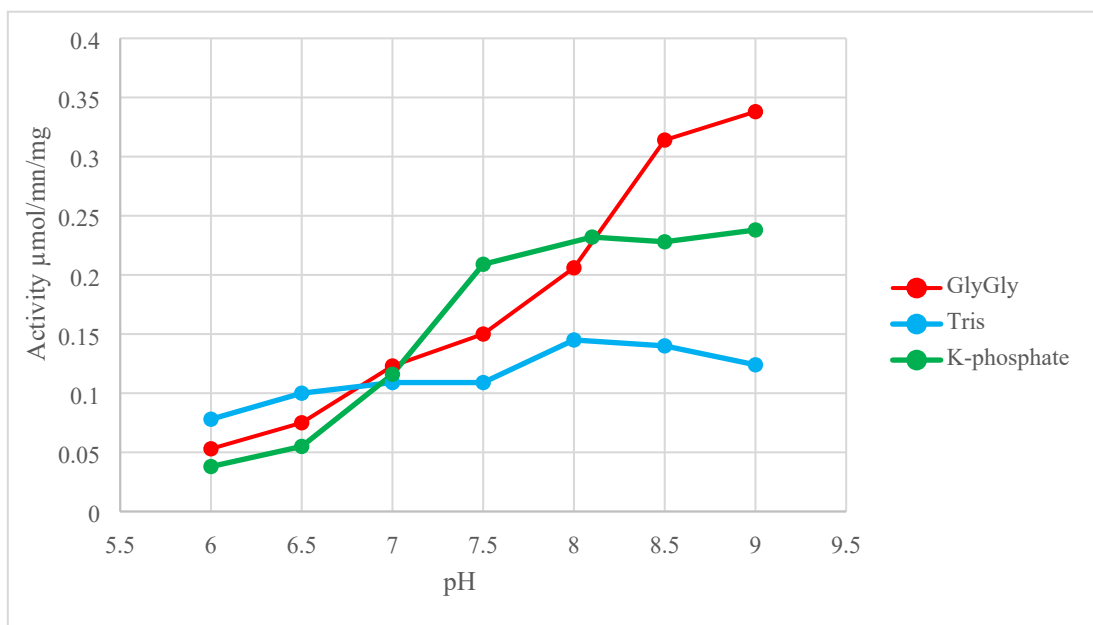


Figure S5 : pH study for FSA<sub>AcAeo</sub>

#### 2.4. Enzyme thermostability

Melting temperatures of FSA<sub>AcAeo</sub>, FSA<sub>AciBac</sub> and FSA<sub>Ecoli</sub> were determined by fluorescence spectroscopy using the protocol described by Life Technologies®. A 125-fold dilution of Protein Thermal Shift™ Dye (fluorophore) was carried out, and Protein Thermal Shift™ Buffer (5µL), then the enzyme solution (12.5 µL *i.e.* 5 µg of FSA<sub>AcAeo</sub> or 62.5µg for FSA<sub>AciBac</sub> and FSA<sub>E.coli</sub>) and Protein Thermal Shift™ Dye (2.5 µL) were added successively to each well in a 96-well plate. The plate was then sealed with MicroAmp® Optical Adhesive Film and shaken at 1000 rpm for 1 min. The plate was then inserted into the Applied Biosystems Real-

Time PCR System. The plate was incubated at 25°C for 2 minutes, then a gradient of 0.05°C/s is applied until 99°C was reached. Fluorescence was measured in real time on a channel with an x4 excitation filter set on  $\lambda = 580 \pm 10$  nm and an m4 emission filter set on  $\lambda = 623 \pm 14$  nm. Melting curves were obtained and once derived, the minimum value gave the  $T_m$ .

For  $FSA_{AcAeo}$ ,  $T_m$  was found at 73°C; for  $FSA_{AcBac}$ ,  $T_m$  of the enzyme was found at 62°C: this first destructure was associated with a loss of enzymatic activity (measured during an additional manipulation) the enzyme then underwent a more significant destructure around 81°C. For  $FSA_{Ecoli}$  the melting temperature was measured at 70°C by this method, in accordance with the literature (established by other methods).

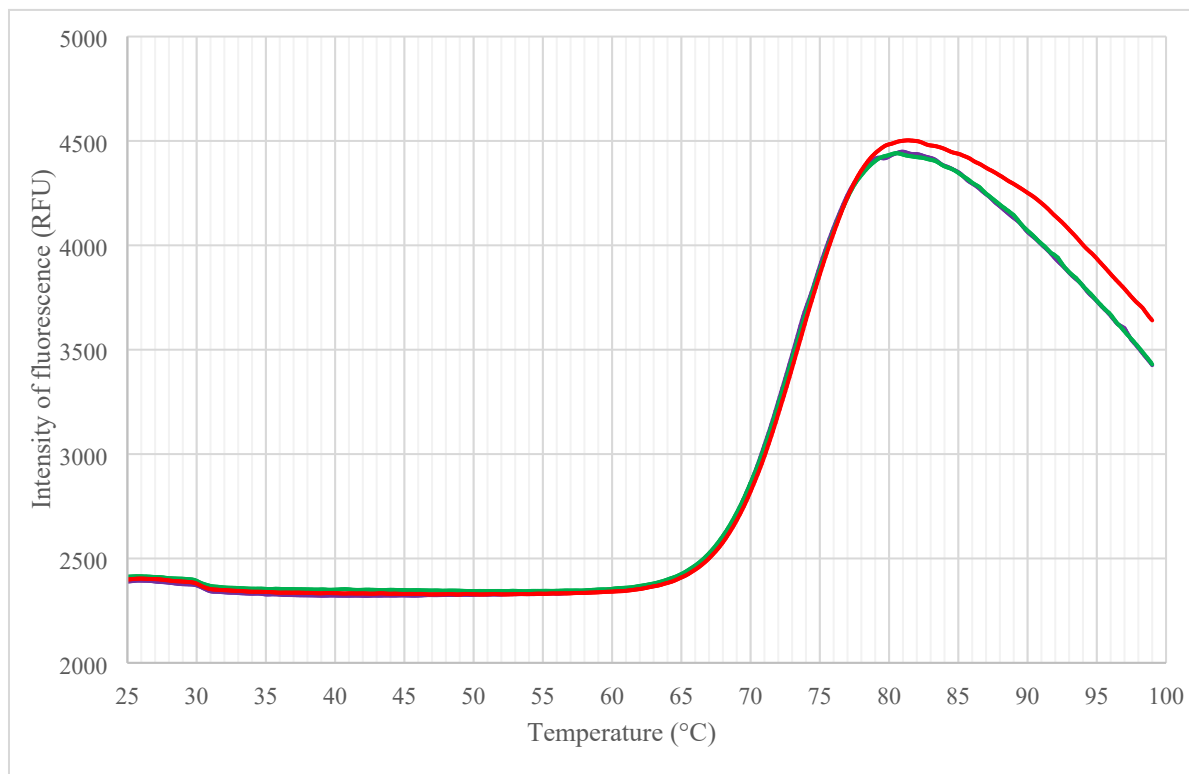


Figure S6 : Melting curve of  $FSA_{AcAeo}$  by measuring fluorescence intensity as a function of temperature, in triplicate

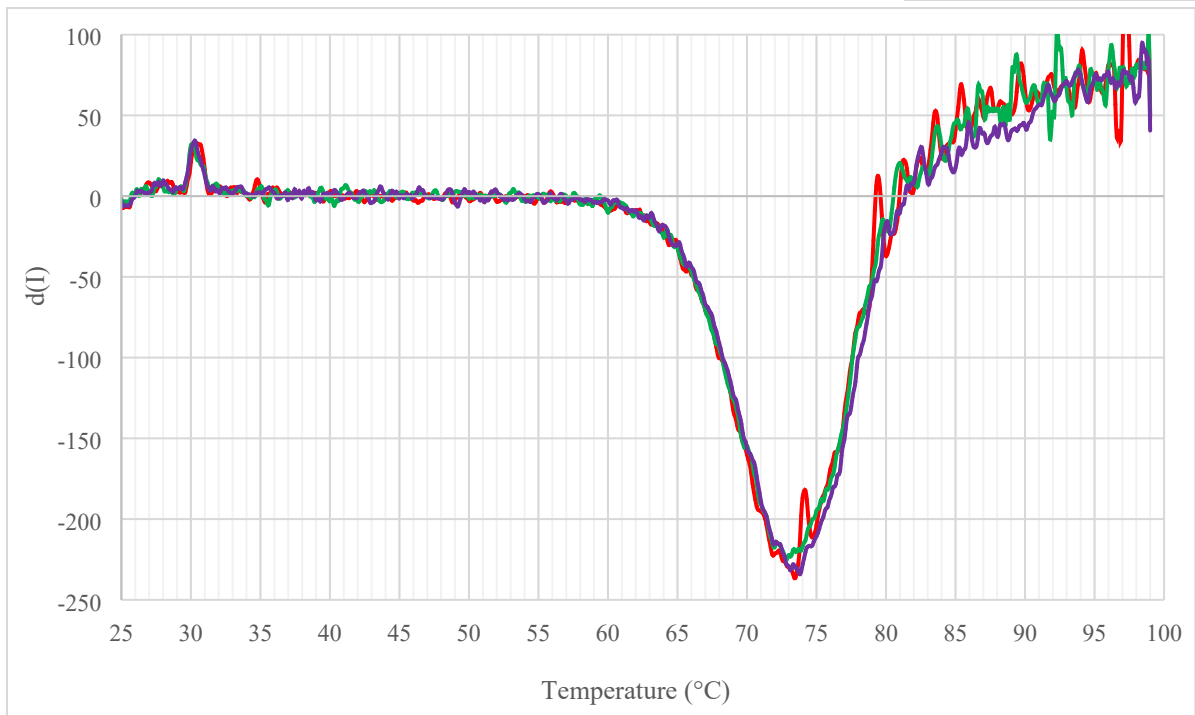


Figure S7 : Derivative of fluorescence intensity for  $FSA_{AcAeo}$  as a function of temperature, in triplicate

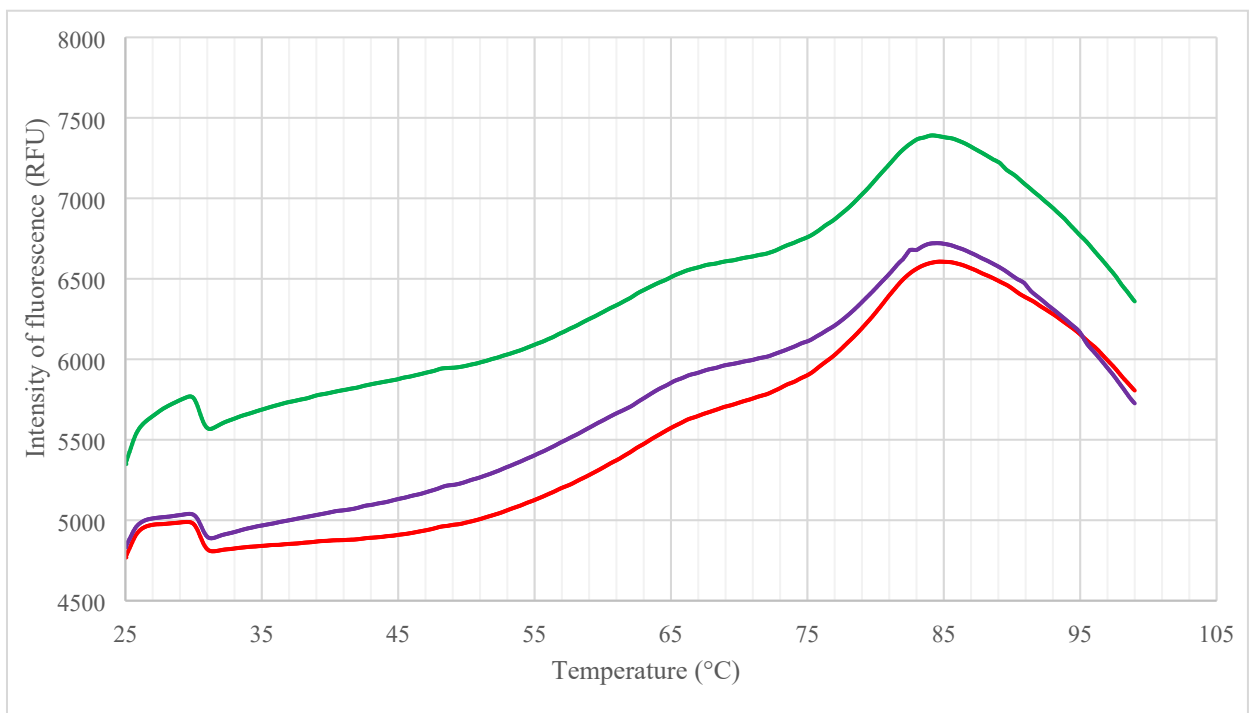


Figure S8 : Melting curve of  $FSA_{AciBac}$  by measuring fluorescence intensity as a function of temperature, in triplicate

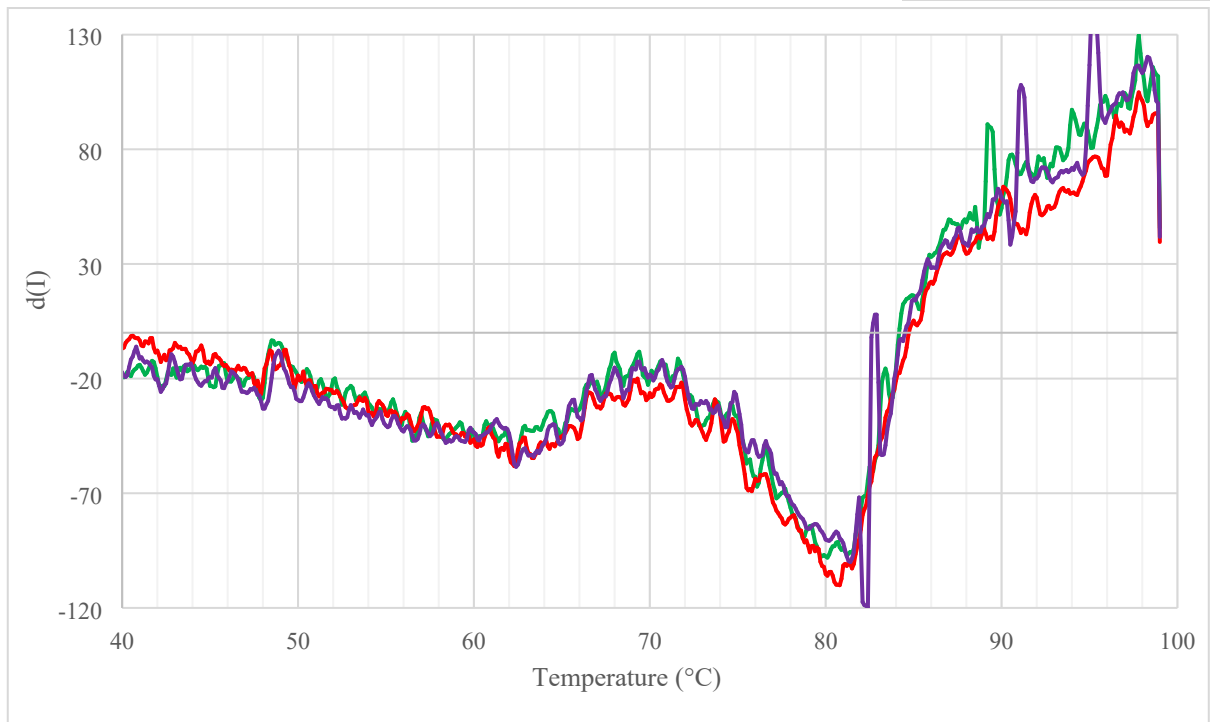


Figure S9 : Derivative of fluorescence intensity for  $FSA_{AciBac}$  as a function of temperature, in triplicate

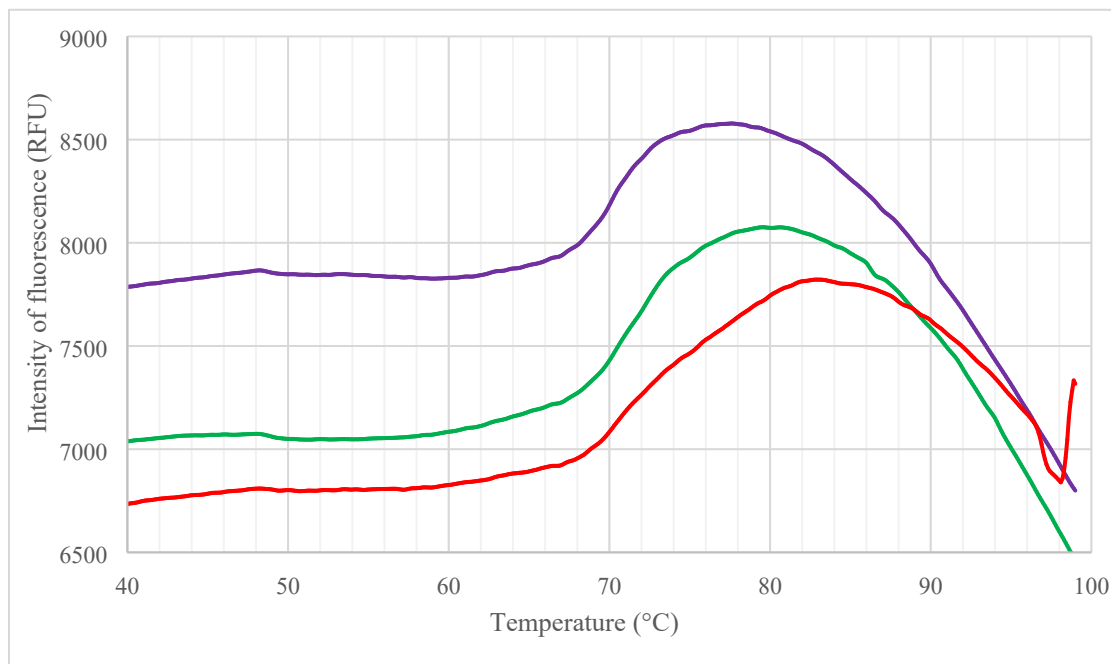


Figure S10 : Melting curve of  $FSA_{Ecoli}$  by measuring fluorescence intensity as a function of temperature, in triplicate.

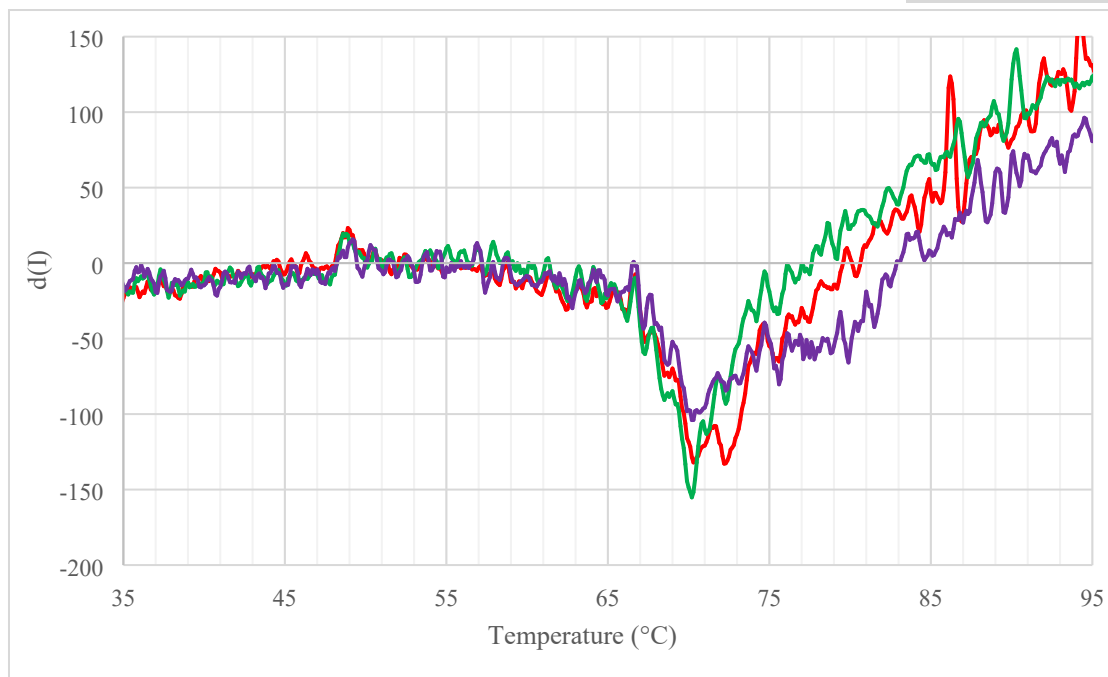


Figure S11 : Derivative of fluorescence intensity for  $FSA_{Ecoli}$  as a function of temperature, in triplicate.

## 2.5. Kinetic constants

FSA kinetics towards D-arabinose-5-phosphate (A5P) or D-arabinose (A) were determined using the same assays as previously described. Each kinetic assay was implemented using 5-300 mM of D-arabinose or 0.2-8 mM of D-arabinose-5-phosphate in glycyglycine buffer 50 mM pH 7.5. with 0.5  $\mu\text{g}$  of  $FSA_{AcBac}$ , 2.5  $\mu\text{g}$  -100  $\mu\text{g}$  of  $FSA_{AcAeo}$  or 0.4  $\mu\text{g}$  -2.0 mg of  $FSA_{Ecoli}$ , the amount of enzyme varying in the last two cases to maintain an enzymatic rate that can be accurately measured with the spectrophotometer.

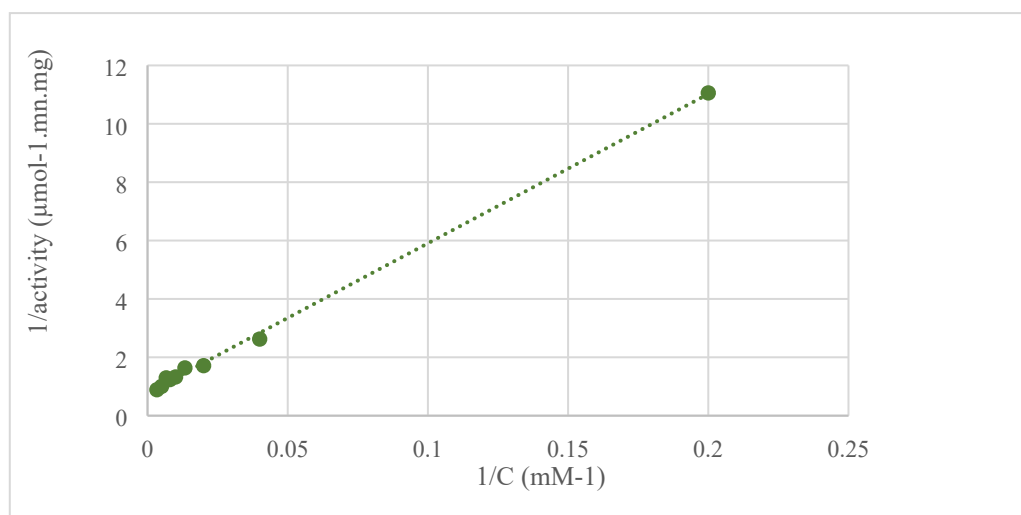


Figure S12 : Lineweaver-Burk plot for  $FSA_{AcAeo}$  with D-arabinose in glycyglycine buffer (pH 7.5, 50 mM)

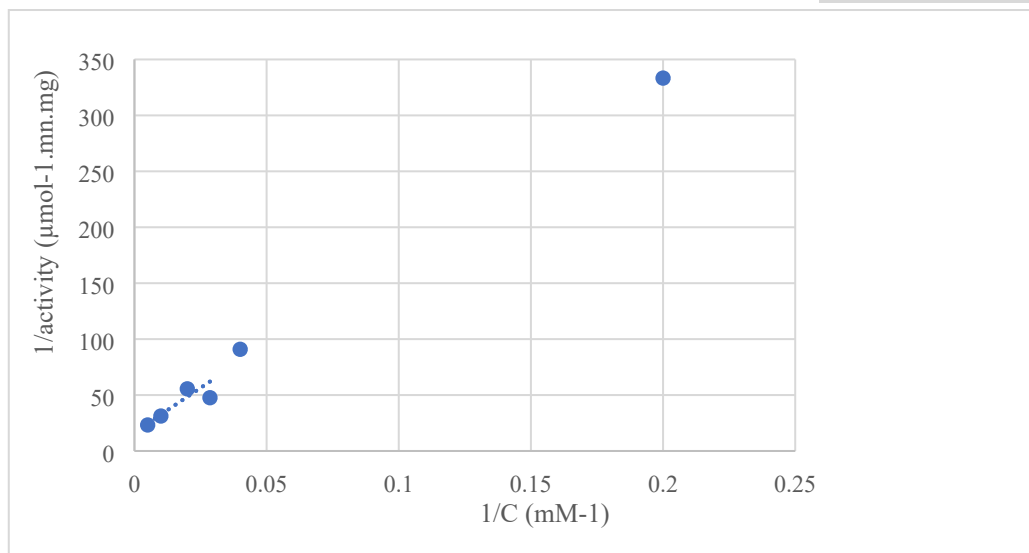


Figure S13 : Lineweaver-Burk plot for FSA<sub>E.coli</sub> with D-arabinose in glycyglycine buffer (pH 7.5, 50 mM)

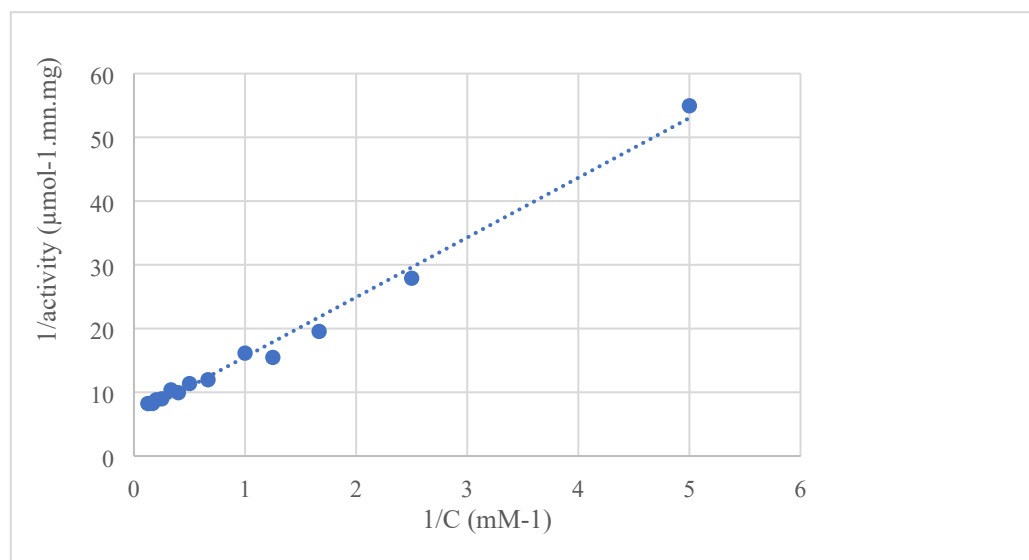


Figure S14 : Lineweaver-Burk plot for FSA<sub>AciBac</sub> with D-arabinose-5-phosphate in glycyglycine buffer (pH 7.5, 50 mM)

## 2.6. Isotopic exchange measurements on nucleophiles by <sup>1</sup>H NMR

To a solution of 2 mg/mL of aldolase (FSA<sub>E.coli</sub>, FSA<sub>AciBac</sub>, FSA<sub>AcAco</sub>) in D<sub>2</sub>O (500 μL) adjusted to pH 7.5, were added 25 μmol (50 mM) of the studied nucleophile. <sup>1</sup>H NMR spectra were recorded after 1 h and 24 h. Activity and selectivity were determined by integration of the signal corresponding to the methylene group of each nucleophile.

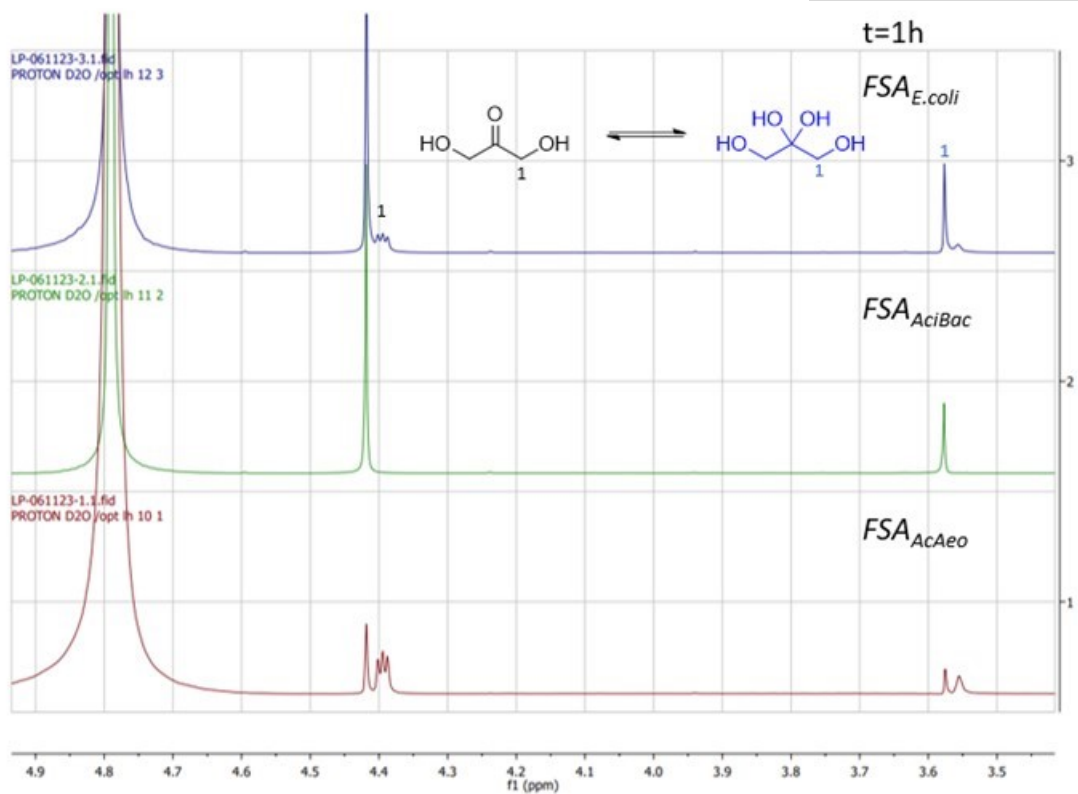


Figure S15 : Isotopic exchange after 1 h for DHA in the presence of  $FSA_{E.coli}$ ,  $FSA_{AciBac}$  and  $FSA_{AcAeo}$

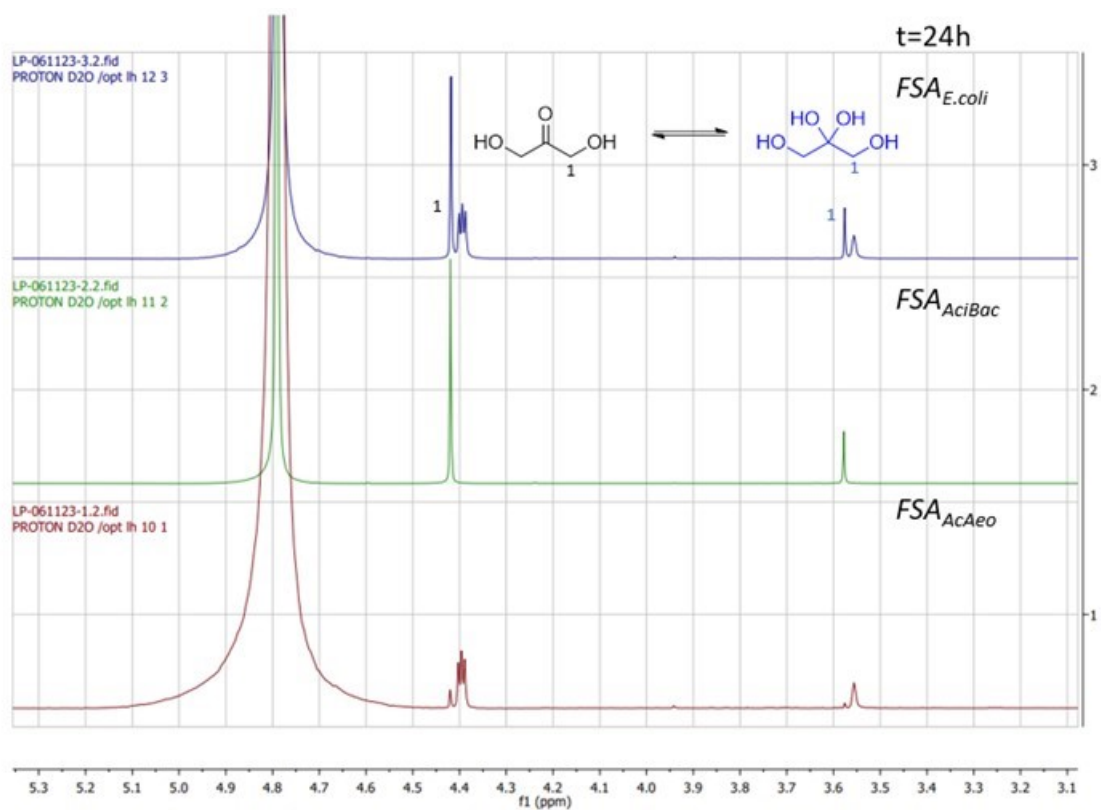


Figure S16 : Isotopic exchange after 24 h for DHA in the presence of  $FSA_{E.coli}$ ,  $FSA_{AciBac}$  and  $FSA_{AcAeo}$

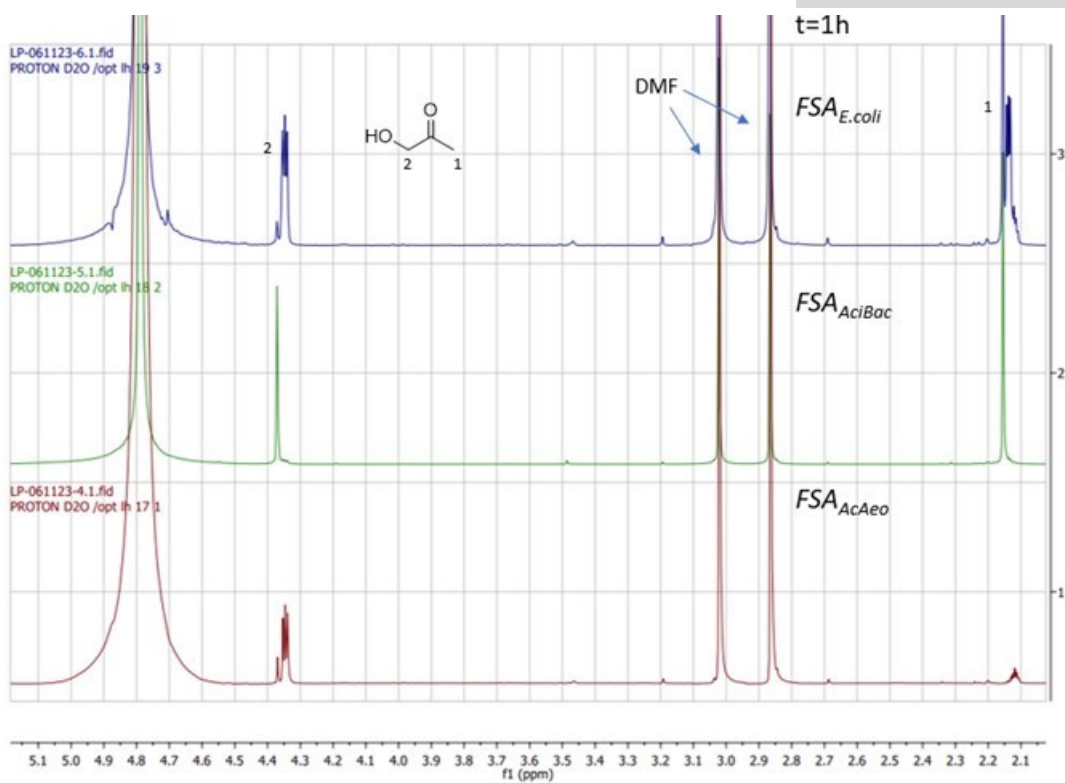


Figure S17 : Isotopic exchange after 1 h for HA in the presence of FSA<sub>E.coli</sub>, FSA<sub>AciBac</sub> and FSA<sub>AcAeo</sub>

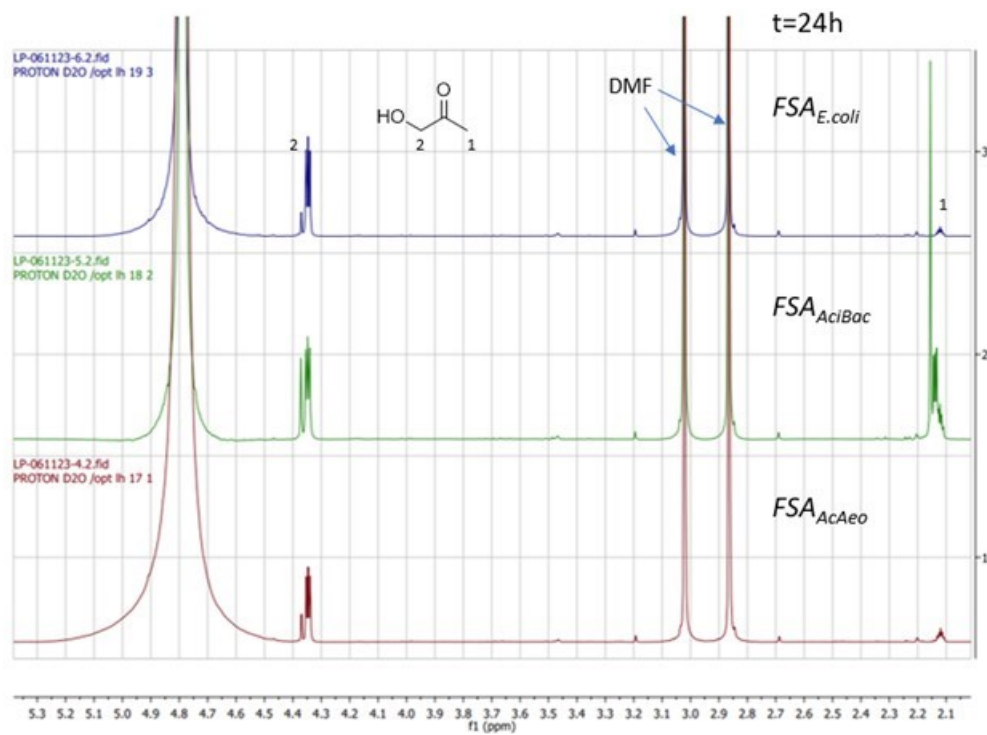


Figure S18 : Isotopic exchange after 24 h for HA in the presence of FSA<sub>E.coli</sub>, FSA<sub>AciBac</sub> and FSA<sub>AcAeo</sub>



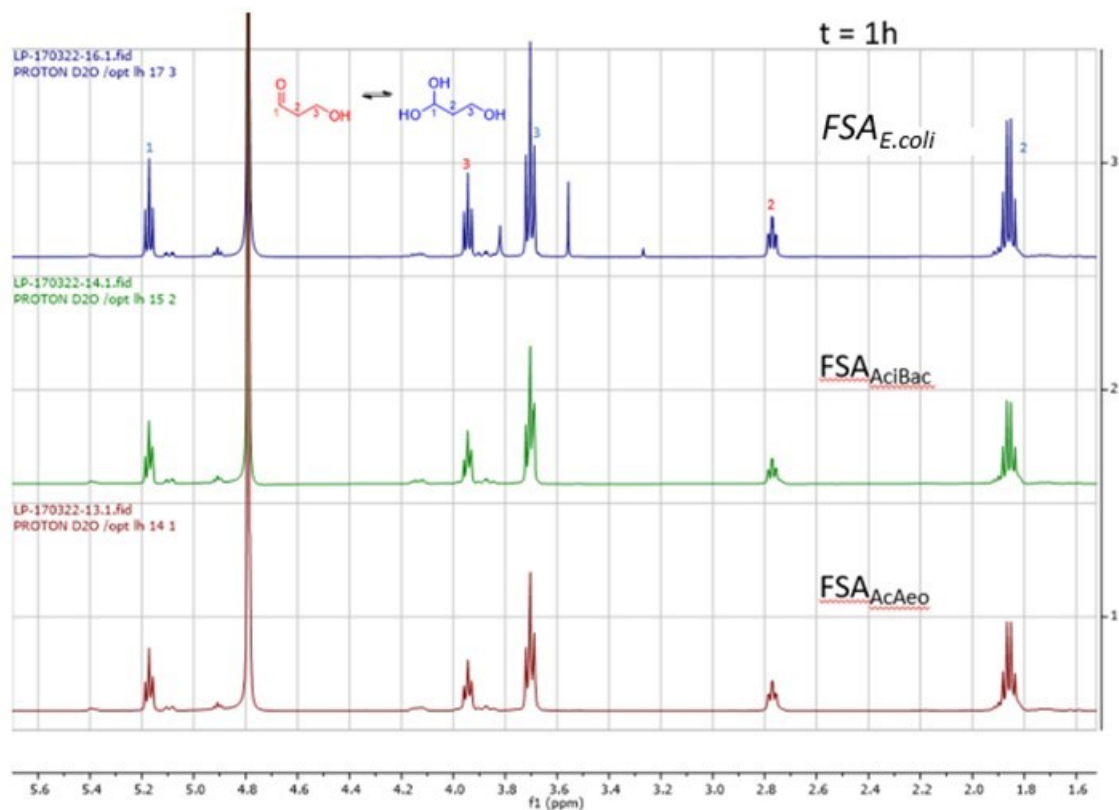


Figure S19 : Isotopic exchange after 1 h for 3-hydroxypropanal in the presence of *FSA<sub>E.coli</sub>*, *FSA<sub>AciBac</sub>* and *FSA<sub>AcAeo</sub>*

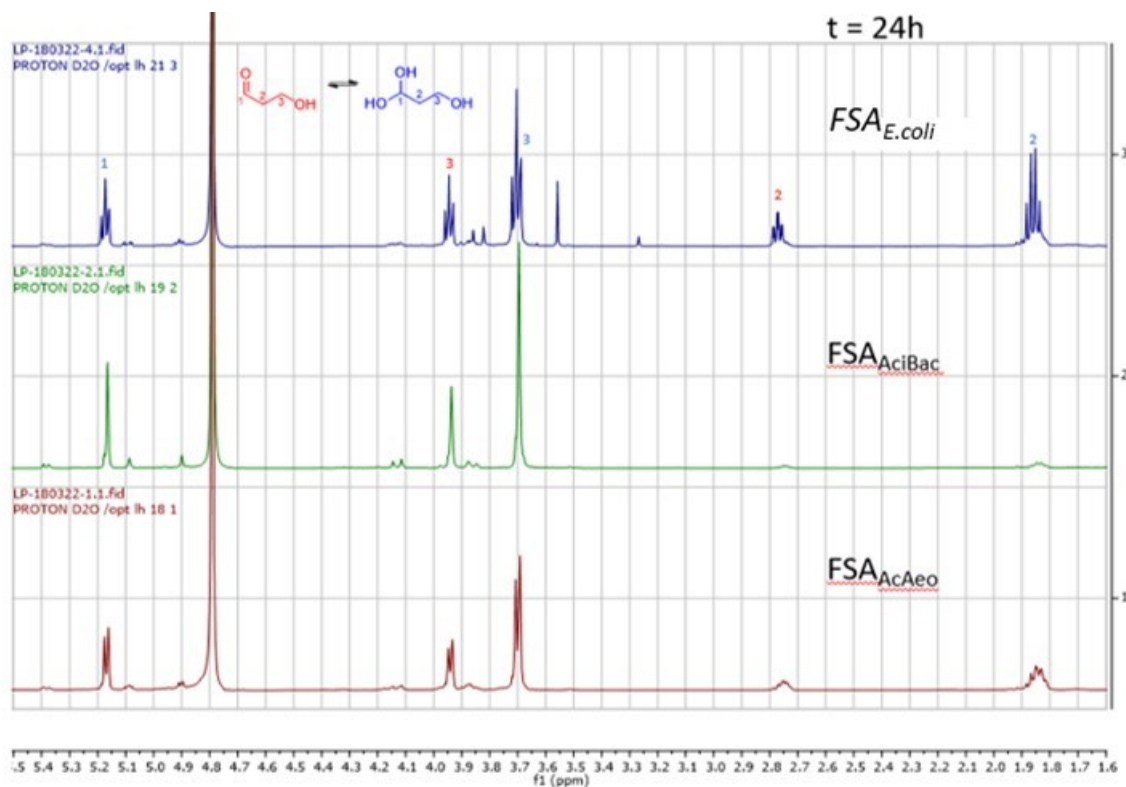


Figure S20 : Isotopic exchange after 24 h for 3-hydroxypropanal in the presence of *FSA<sub>E.coli</sub>*, *FSA<sub>AciBac</sub>* and *FSA<sub>AcAeo</sub>*

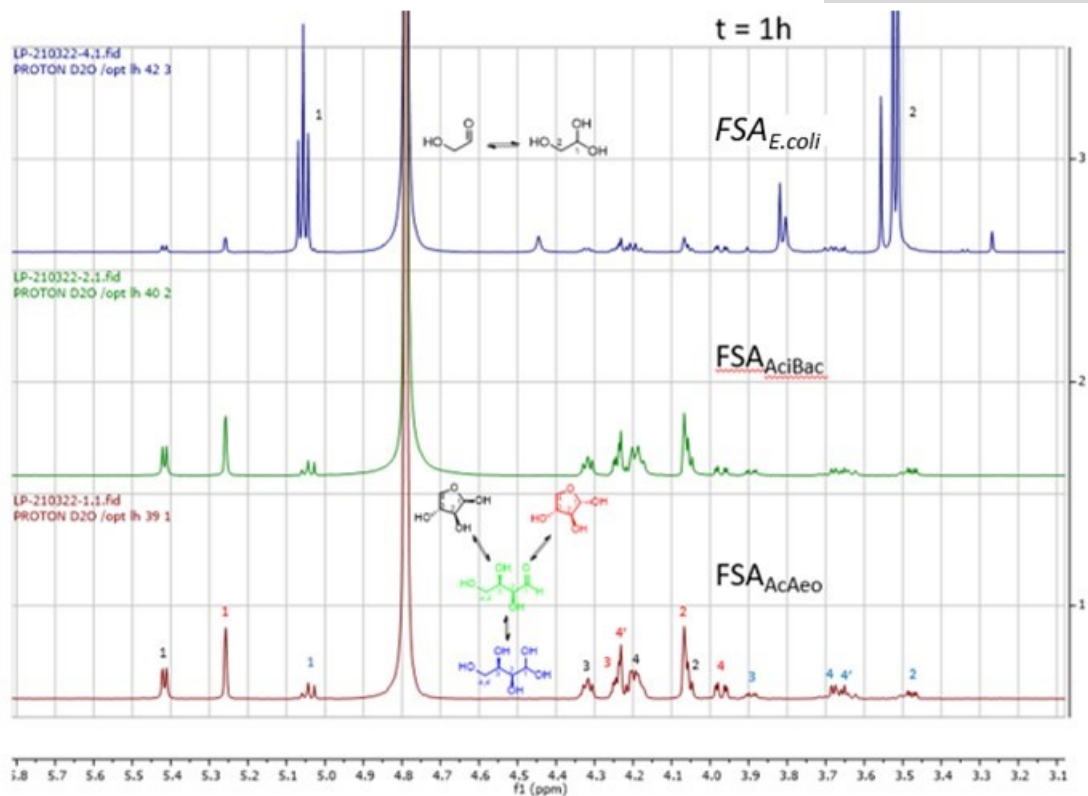


Figure S21 : Isotopic exchange after 1 h for glycolaldehyde in the presence of FSA<sub>E.coli</sub>, FSA<sub>AciBac</sub> and FSA<sub>AcAeo</sub>

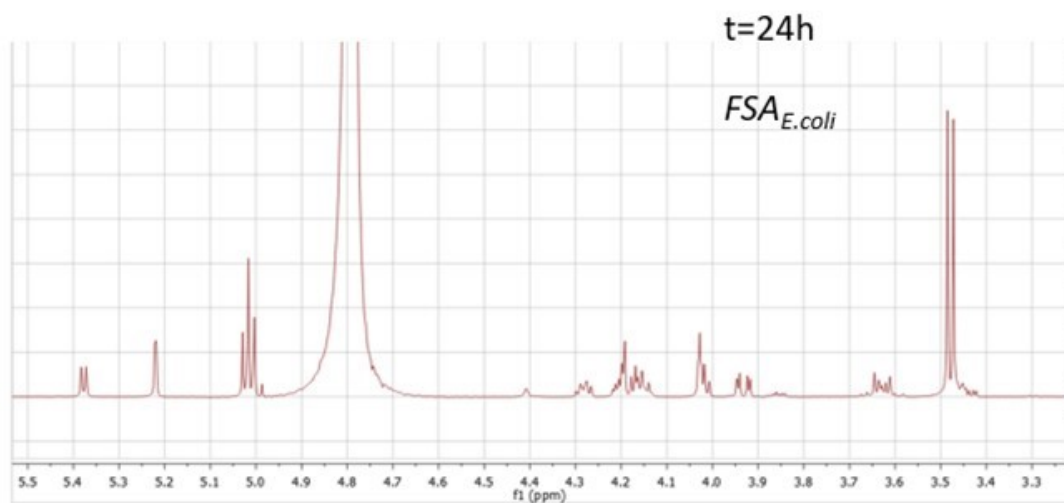


Figure S22 : Isotopic exchange after 24 h for glycolaldehyde in the presence of FSA<sub>E.coli</sub>

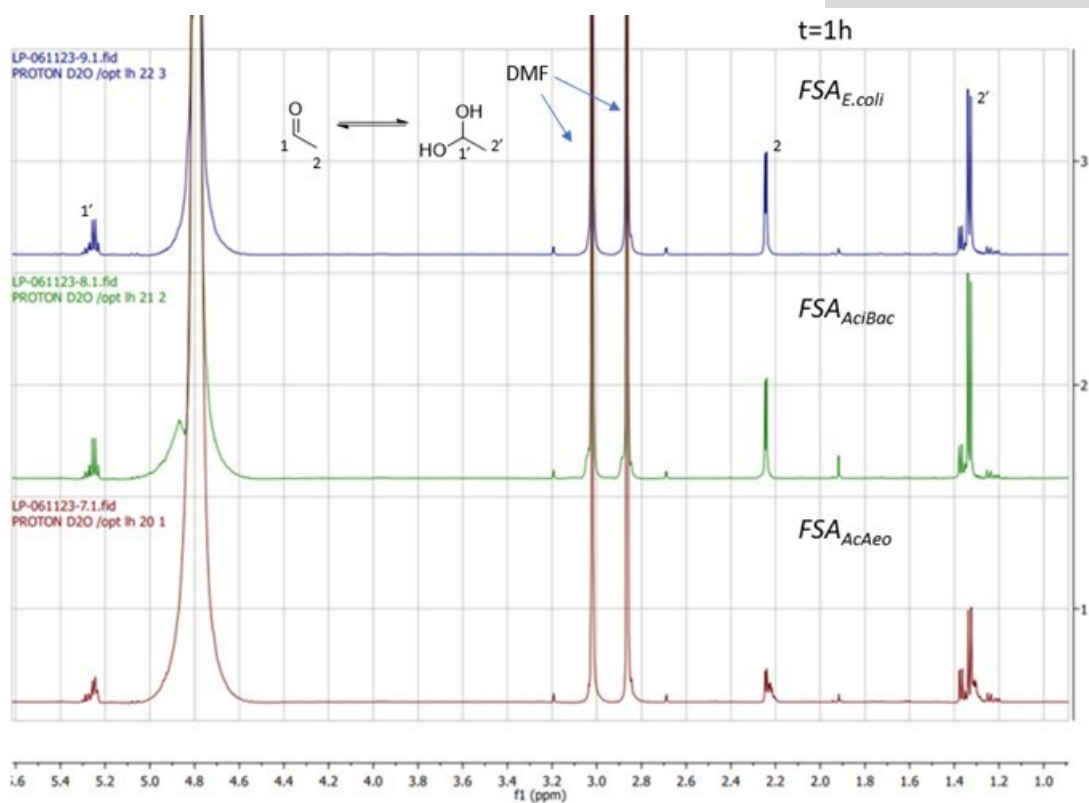


Figure S23 : Isotopic exchange after 1 h for acetaldehyde in the presence of *FSA<sub>E.coli</sub>*, *FSA<sub>AciBac</sub>* and *FSA<sub>AcAeo</sub>*

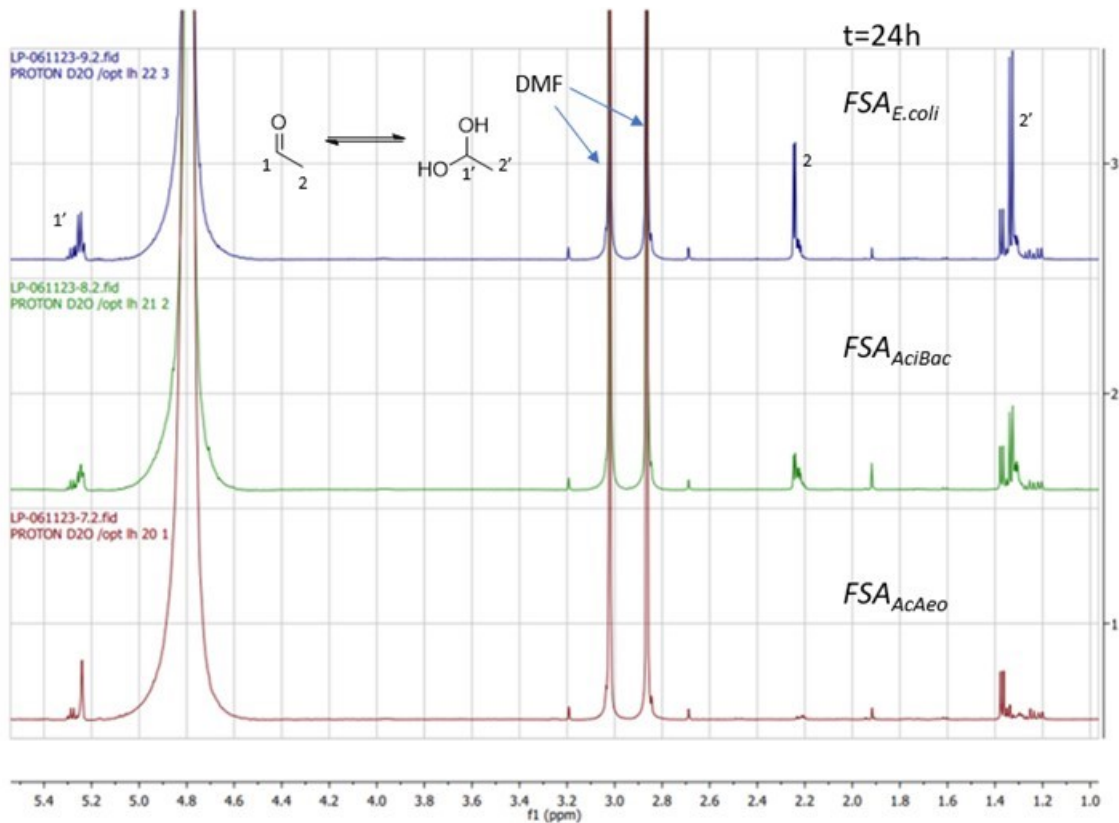


Figure S24 : Isotopic exchange after 24 h for acetaldehyde in the presence of *FSA<sub>E.coli</sub>*, *FSA<sub>AciBac</sub>* and *FSA<sub>AcAeo</sub>*

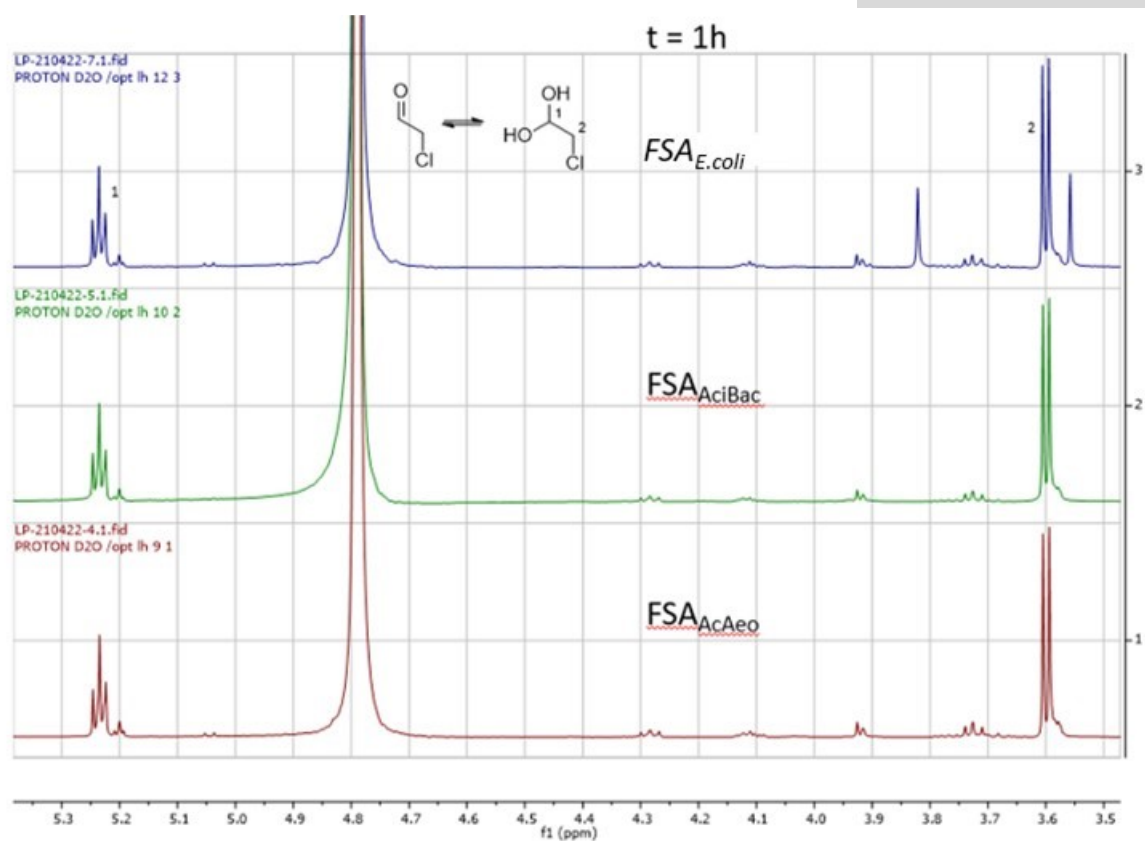


Figure S25 : Isotopic exchange after 1 h for chloroacetaldehyde in the presence of *FSA<sub>E.coli</sub>*, *FSA<sub>AciBac</sub>* and *FSA<sub>AcAeo</sub>*

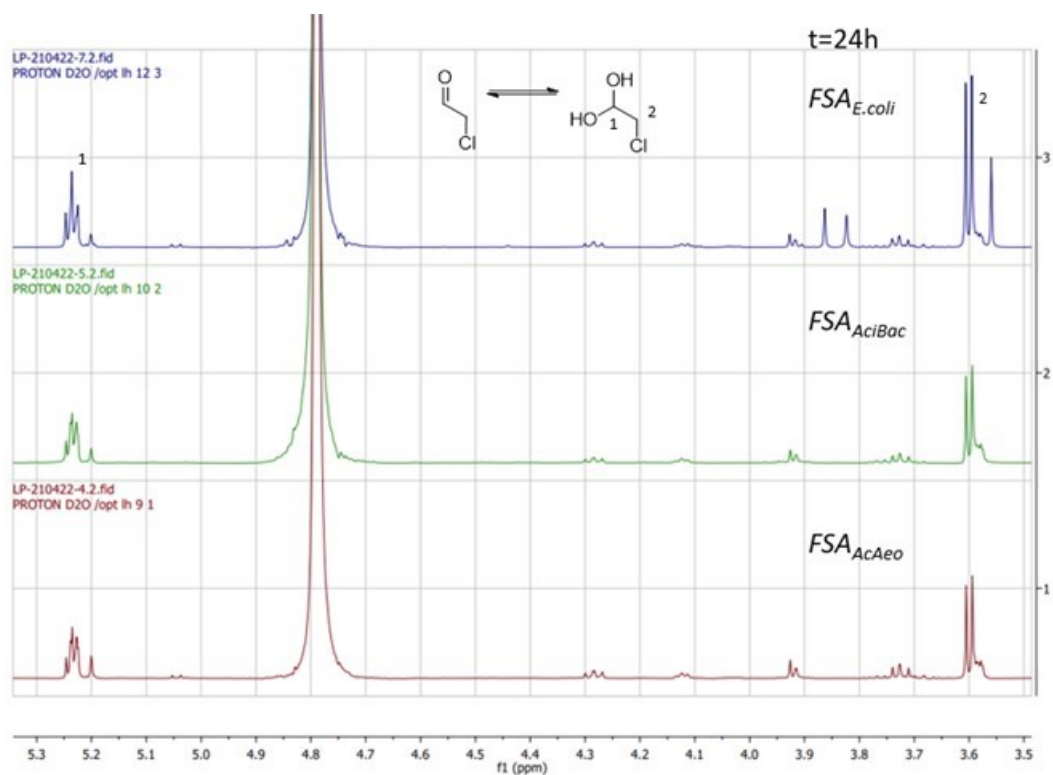


Figure S26 : Isotopic exchange after 24 h for chloroacetaldehyde in the presence of *FSA<sub>E.coli</sub>*, *FSA<sub>AciBac</sub>* and *FSA<sub>AcAeo</sub>*

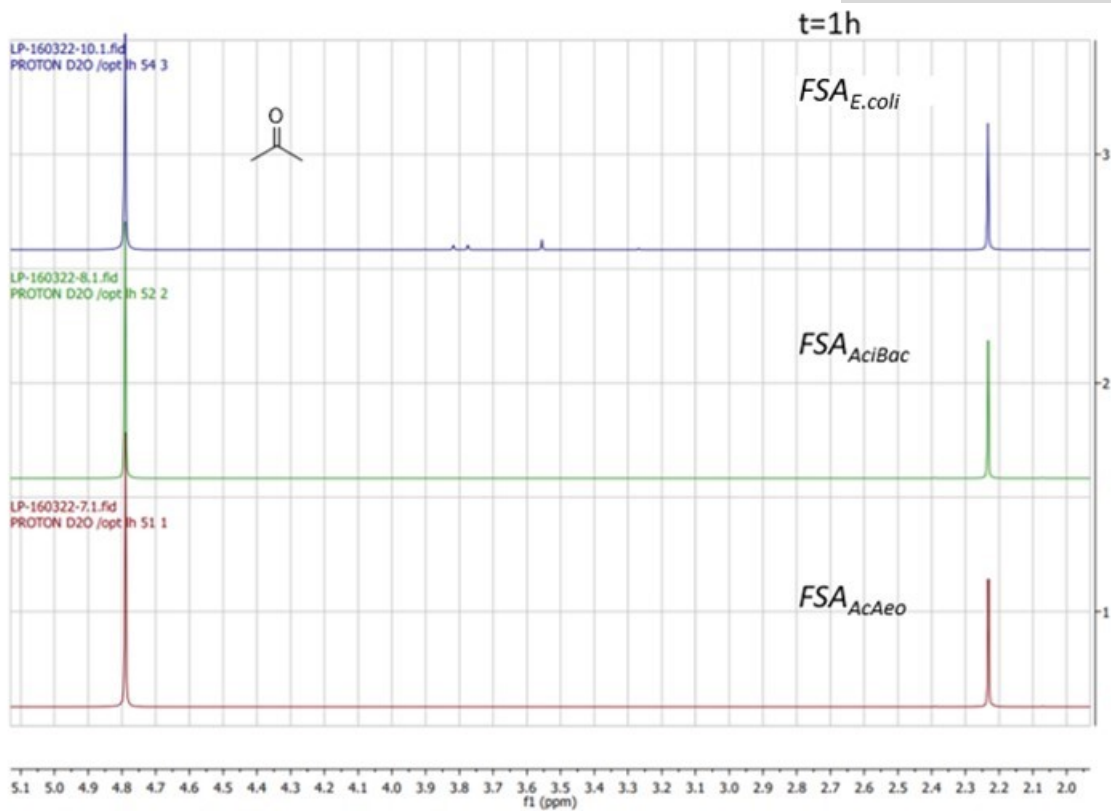


Figure S27 : Isotopic exchange after 1 h for acetone in the presence of  $\text{FSA}_{E.coli}$ ,  $\text{FSA}_{AciBac}$  and  $\text{FSA}_{AcAeo}$

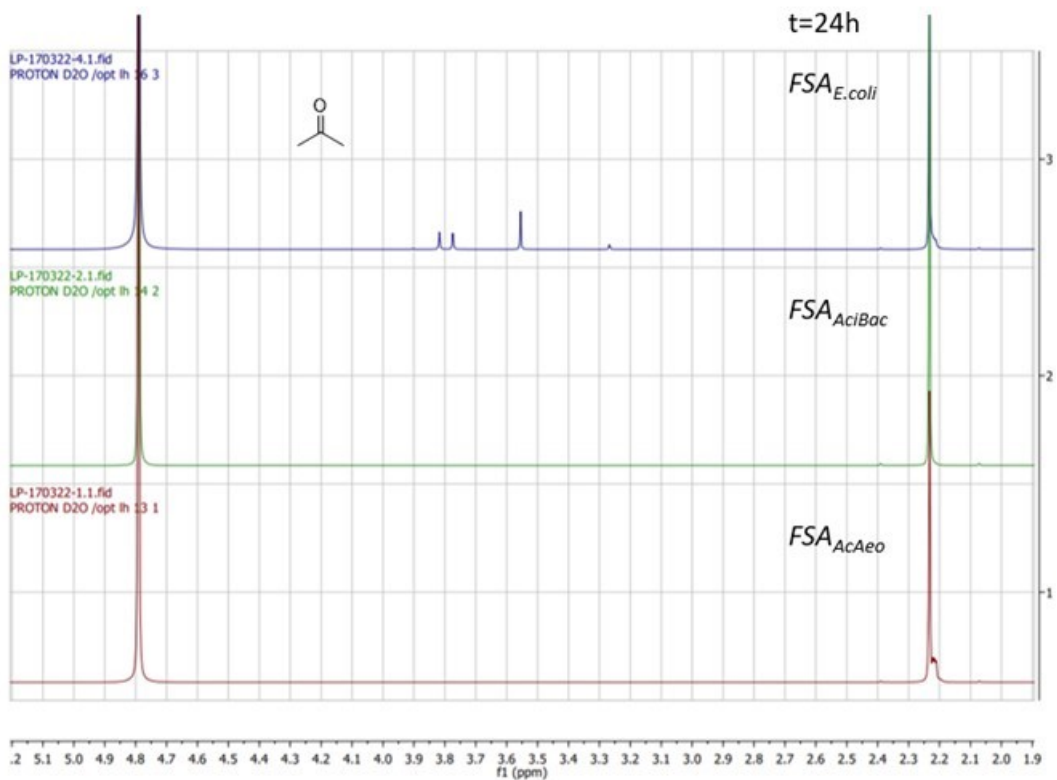


Figure S28 : Isotopic exchange after 24 h for acetone in the presence of  $\text{FSA}_{E.coli}$ ,  $\text{FSA}_{AciBac}$  and  $\text{FSA}_{AcAeo}$

### 3. Molecular modelling

#### 3.1. Construction of the structures

Structures (Resolution, date)	A0A399XY01: FSA <sub>AcBac</sub> percent identity	A0A0Q0RVA3: FSA <sub>AcAeo</sub> percent identity	Organism	Publications (DOI)
1L6W (1.93, 2002) <sup>4</sup>	26.9	26.8	<i>Escherichia coli</i>	10.1016/S0022-2836(02)00258-9
1VPX (2.40, 2004)	29.2	36.0	<i>Thermotoga maritima</i>	To be published.
1WX0 (2.27, 2005)	31.0	31.8	<i>Thermoplasma acidophilum</i> DSM 1728	
3SOC (1.78, 2011) <sup>5</sup>	28.2	42.2	<i>Thermoplasma acidophilum</i> DSM 1728	10.1038/nchembio.633
3S1U (1.90, 2011)	28.2	42.2	<i>Thermoplasma acidophilum</i> DSM 1728	
3S1V (1.80, 2011)	28.2	42.2	<i>Thermoplasma acidophilum</i> DSM 1728	
3S1X (1.65, 2011)	28.2	42.2	<i>Thermoplasma acidophilum</i> DSM 1728	
3S1W (1.80, 2011, K86A)	27.8	41.7	<i>Thermoplasma acidophilum</i> DSM 1728	
3R8R (1.90, 2011) <sup>6</sup>	31.1	34.4	<i>Bacillus subtilis</i>	10.1111/j.1742-4658.2011.08467.x
4RXF (2.40, 2014, Y131F) <sup>7</sup>	25.9	25.3	<i>Escherichia coli K-12</i>	10.1002/cctc.201500478
4RZ4 (1.75, 2014, Q59E, Y131F)	25.5	24.9	<i>Escherichia coli K-12</i>	
4RXG (2.15, 2014)	26.4	26.4	<i>Escherichia coli K-12</i>	
4S1F (2.24, 2015)	26.4	25.8	<i>Escherichia coli K-12</i>	
4XZ9 (1.80, 2015) <sup>8</sup>	29.2	43.1	<i>Thermoplasma acidophilum</i> DSM 1728	10.1021/acs.biochem.5b00283
5ZOL (2.17, 2018, I31T, Q59T, I195Q) <sup>9</sup>	26.4	25.3	<i>Escherichia coli K-12</i>	10.1039/d0cc02437f
6YR3 (1.48, 2020)	28.2	42.2	<i>Thermoplasma acidophilum</i> DSM 1728	To be published
6YS0 (1.70, 2020, D211A)	28.7	41.7	<i>Thermoplasma acidophilum</i> DSM 1728	
6YRT (1.65, 2020, T30D)	28.2	42.2	<i>Thermoplasma acidophilum</i> DSM 1728	
6YRM (1,70, 2020, T30A)	28.2	42.2	<i>Thermoplasma acidophilum</i> DSM 1728	
6YRE (1.96, 2020, T30C, D211C)	28.2	42.2	<i>Thermoplasma acidophilum</i> DSM 1728	
6YRH (1.80, 2020, T30C, D211C)	28.2	42.2	<i>Thermoplasma acidophilum</i> DSM 1728	

Table 3. 21 protein sequences found from the PDB after Basic Local Alignment with FSA<sub>AcBac</sub> and FSA<sub>AcAeo</sub> using Chimera software.

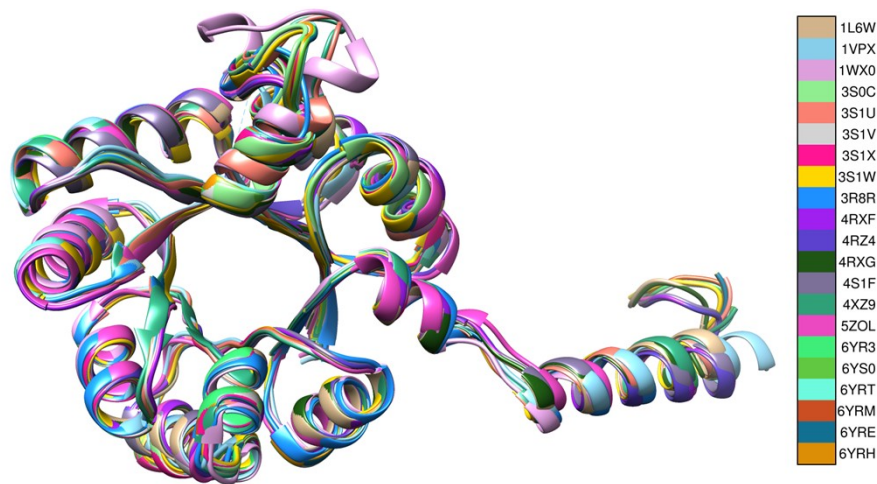


Figure S29. Superimposition of the 21 proteins showing an identical ( $\beta/\alpha$ ) 8-barrel fold secondary structure near the reactive lysine and a Cter alpha helix varying in length.

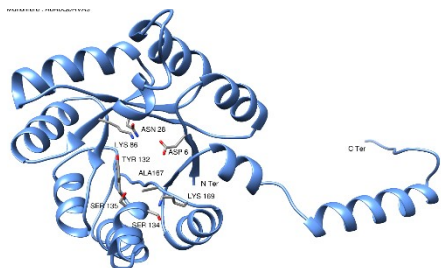


Figure S30. Proposed structure for FSA<sub>AcAeo</sub>

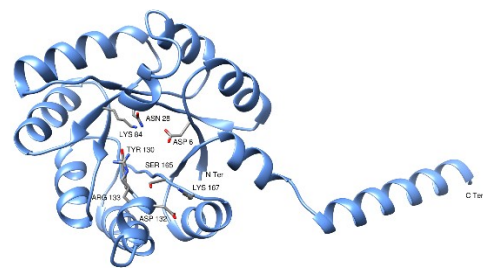


Figure S31. Proposed structure for FSA<sub>AciBac</sub>

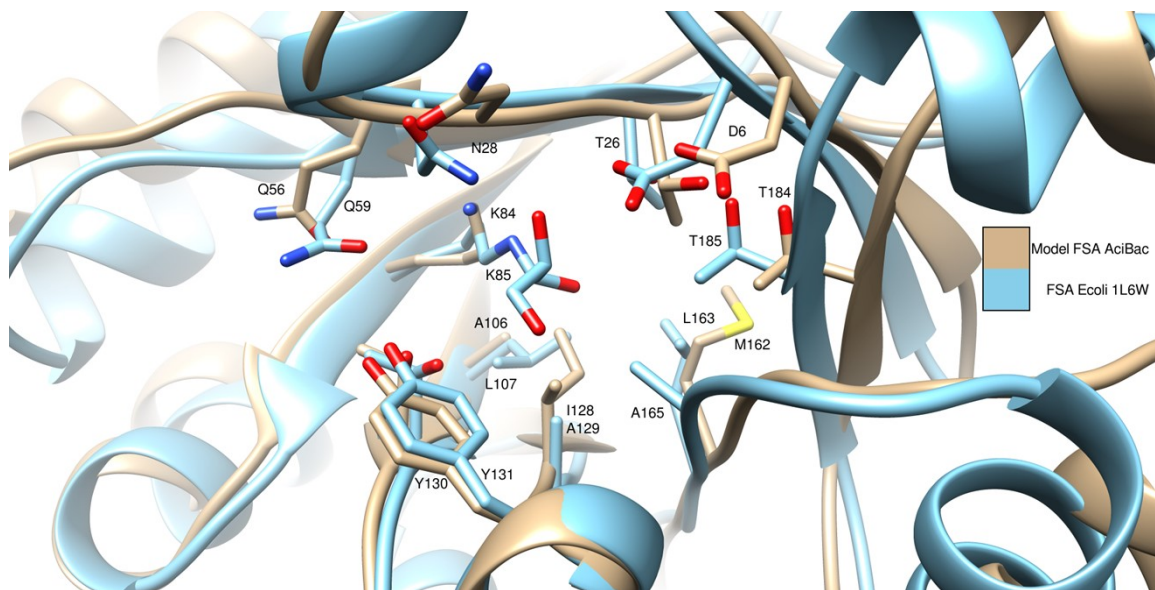


Figure S32. Superimposition of 1L6W crystallographic structure of FSA<sub>Ecoli</sub> in blue with our model structure of FSA<sub>AciBac</sub> in brown determined using Modeller 10.4,<sup>10</sup> Chimera 1.17.1<sup>11</sup> and AlphaFold<sup>12</sup>.

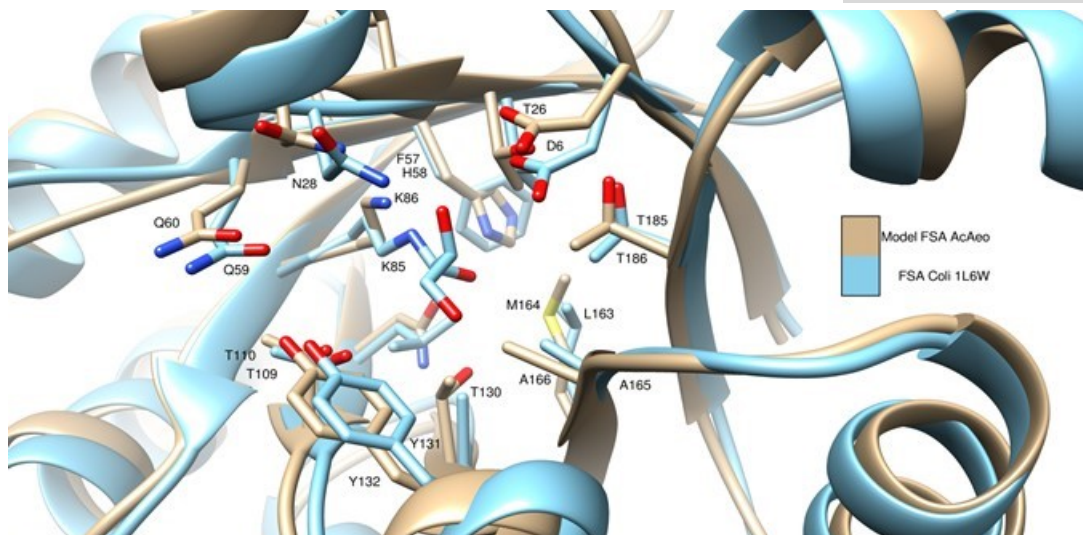


Figure S33. Superimposition of 1L6W crystallographic structure of  $FSA_{Ecoli}$  in blue with our model structure of  $FSA_{AcAeo}$  in brown.

### 3.2. Docking experiments

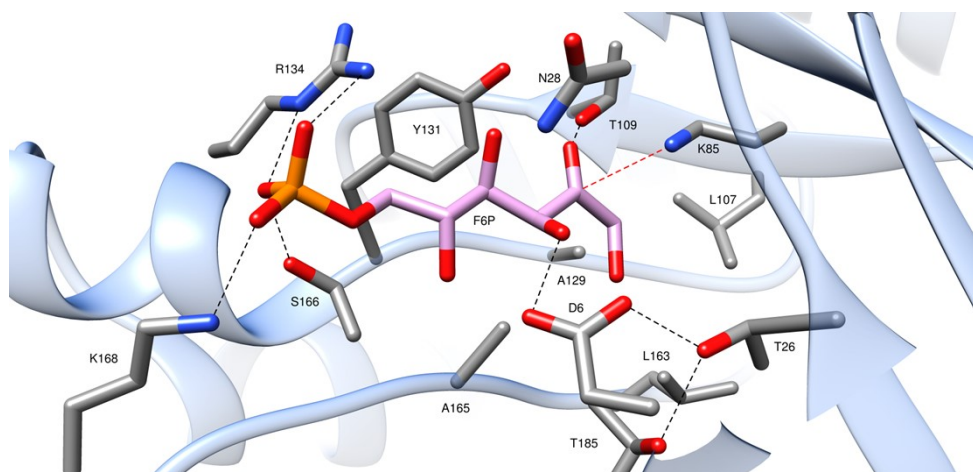


Figure S34. Docking of fructose-6-phosphate (pink) in  $FSA_{Ecoli}$  active site with Autodock 4.2™,<sup>13</sup> leading to a binding energy of -8.5 kcal/mol for the best solution over 500 belonging to a same cluster, and an estimated  $K_i$  of 572 nM.



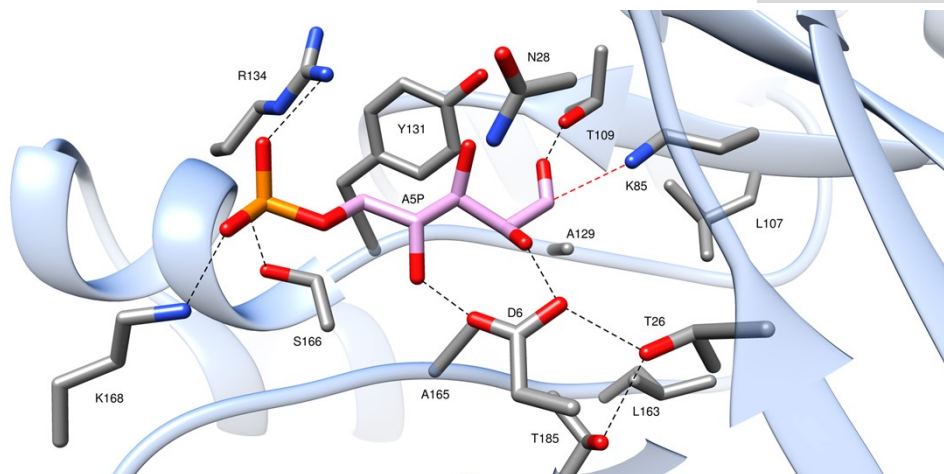


Figure S35. Docking of arabinose-5-phosphate (pink) in  $FSA_{Ecoli}$  active site with Autodock 4.2™, leading to a binding energy of -8.9 kcal/mol for the best solution over 500 belonging to a same cluster, and an estimated  $K_i$  of 322 nM.

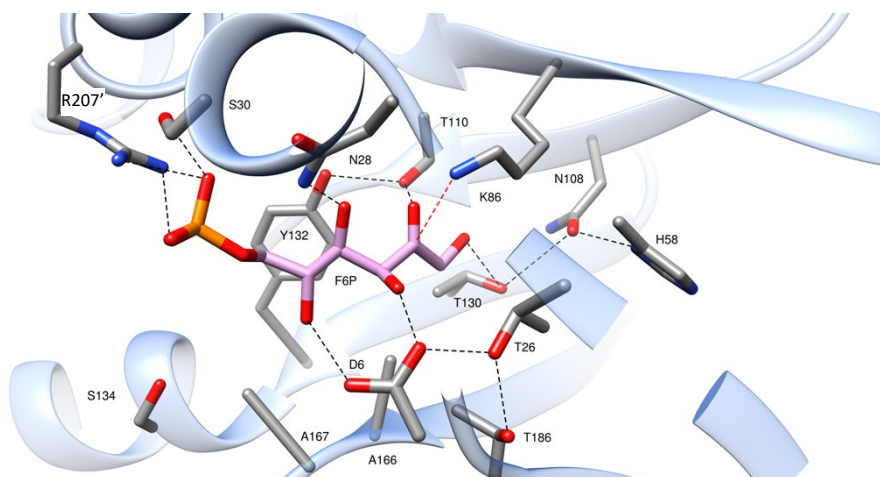


Figure S36. Docking of fructose-6-phosphate (pink) in  $FSA_{AcAeo}$  active site with Autodock 4.2™, leading to a binding energy of -5.7 kcal/mol for the best solution over 497 belonging to a same cluster, and an estimated  $K_i$  of 65  $\mu$ M.

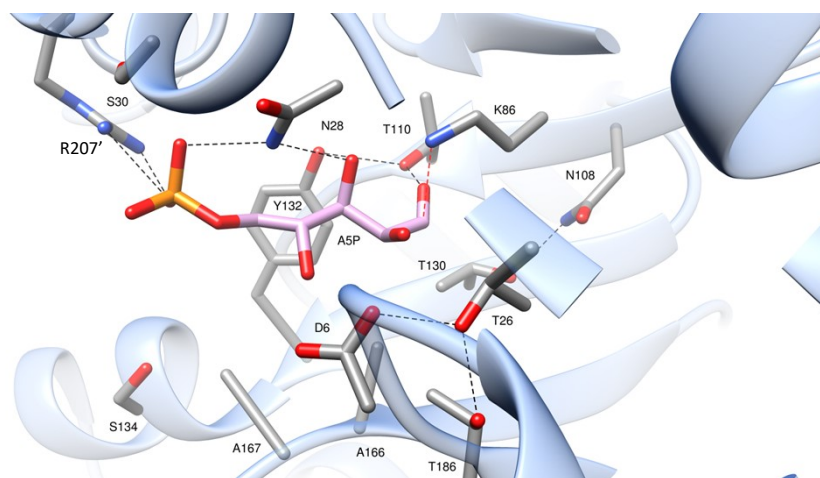


Figure S37. Docking of arabinose-5-phosphate (pink) in  $FSA_{AcAeo}$  active site with Autodock 4.2™, leading to a binding energy of -5.6 kcal/mol for the best solution over 500 belonging to a same cluster, and an estimated  $K_i$  of 75  $\mu$ M.

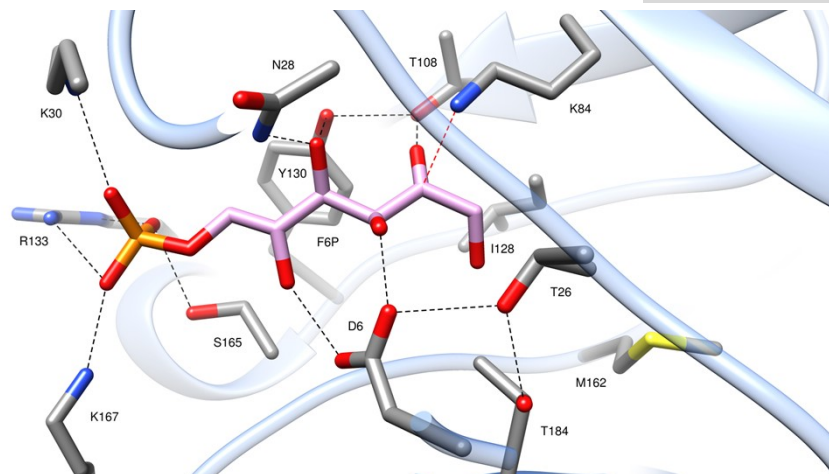


Figure S38. Docking of fructose-6-phosphate (pink) in  $FSA_{AciBac}$  active site with Autodock 4.2™, leading to a binding energy of -7.7 kcal/mol for the best solution over 494 belonging to a same cluster, and an estimated  $K_i$  of 2.3  $\mu$ M.

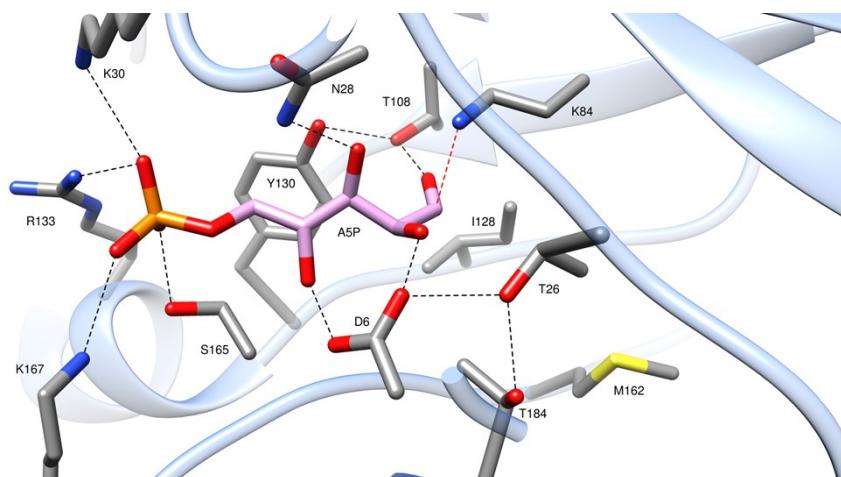


Figure S39. Docking of arabinose-5-phosphate (pink) in  $FSA_{AciBac}$  active site with Autodock 4.2™, leading to a binding energy of -8.3 kcal/mol for the best solution over 500 belonging to a same cluster, and an estimated  $K_i$  of 781 nM.

#### 4. Electrophiles study

40 mM of hydroxyacetone (HA) and 60 mM of the studied electrophile in solution in water at pH 7.5 were placed in a vial, a blank was collected and 2 mg of enzyme ( $FSA_{AcAeo}$ ,  $FSA_{AciBac}$  or  $FSA_{Ecoli}$ ) were added. Samples were taken at regular intervals and HA content was determined using glycerol dehydrogenase, allowing spectroscopic monitoring of the reaction at 340 nm.

#### 5. Syntheses

##### 5.1. D-threose from glycolaldehyde

150 mg (500 mM) of GoA in solution in 5 mL of water were placed in a vial. The pH of the medium was adjusted to 8.3 and 10 mg of  $FSA_{AciBac}$  were added. In parallel, for comparison,

60 mg of GoA (500 mM) in solution in 2 mL of water were placed in a vial and the pH of the medium was adjusted to 8.4 and 4.2 mg of FSA<sub>Ecoli</sub> were then added. The reactions were stirred at room temperature. The reaction was complete after 4 h for FSA<sub>AciBac</sub> whereas for FSA<sub>Ecoli</sub> the reaction was almost complete after 24 h (see NMR spectrum). After completion, FSA<sub>AciBac</sub> was discarded via IMAC technique. The pH was then adjusted to 5 and the mixture was freeze-dried. 151.8 mg of a crystalline solid was obtained. The reaction was quantitative, the product containing 2 mg of salts due to the addition of sodium hydroxide and HCl to balance the pH.

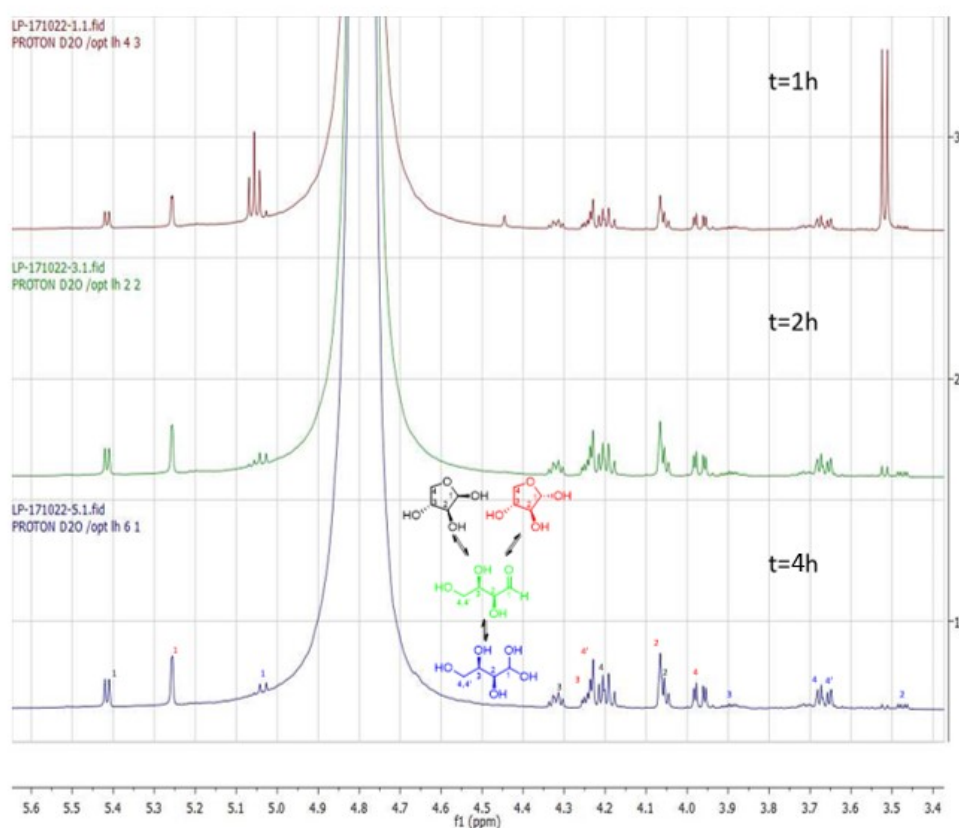


Figure S40 : <sup>1</sup>H NMR monitoring of D-threose formation with FSA<sub>AciBac</sub>

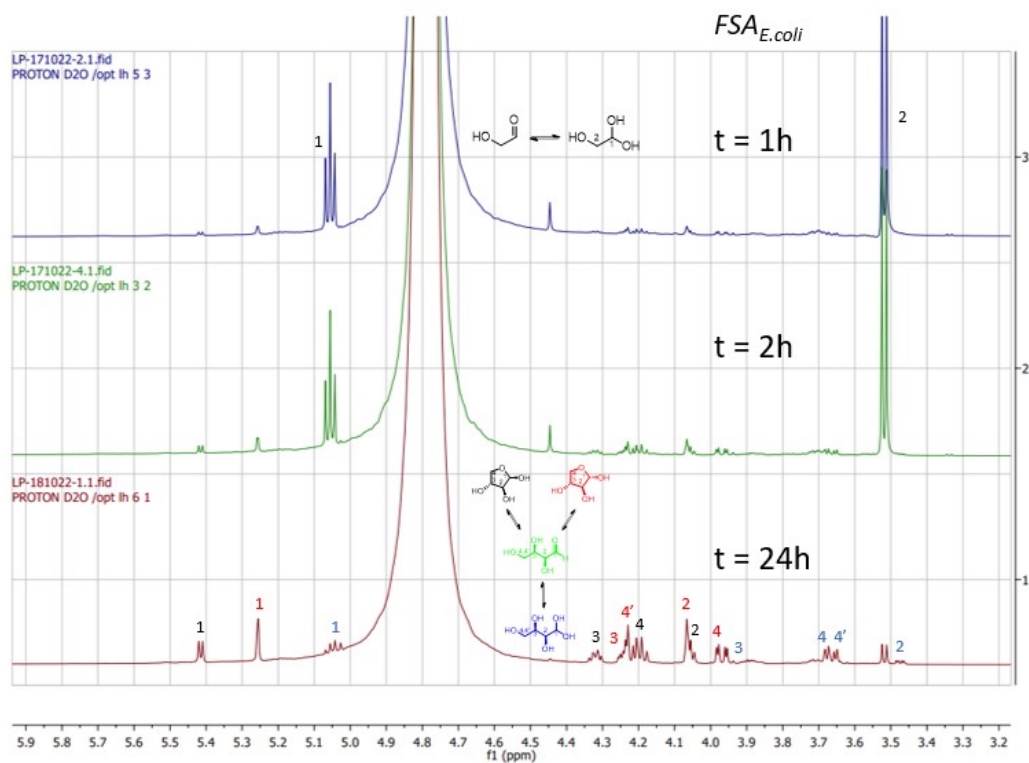


Figure S41 :  $^1\text{H}$  NMR monitoring of D-threose formation with FSA<sub>E.coli</sub>

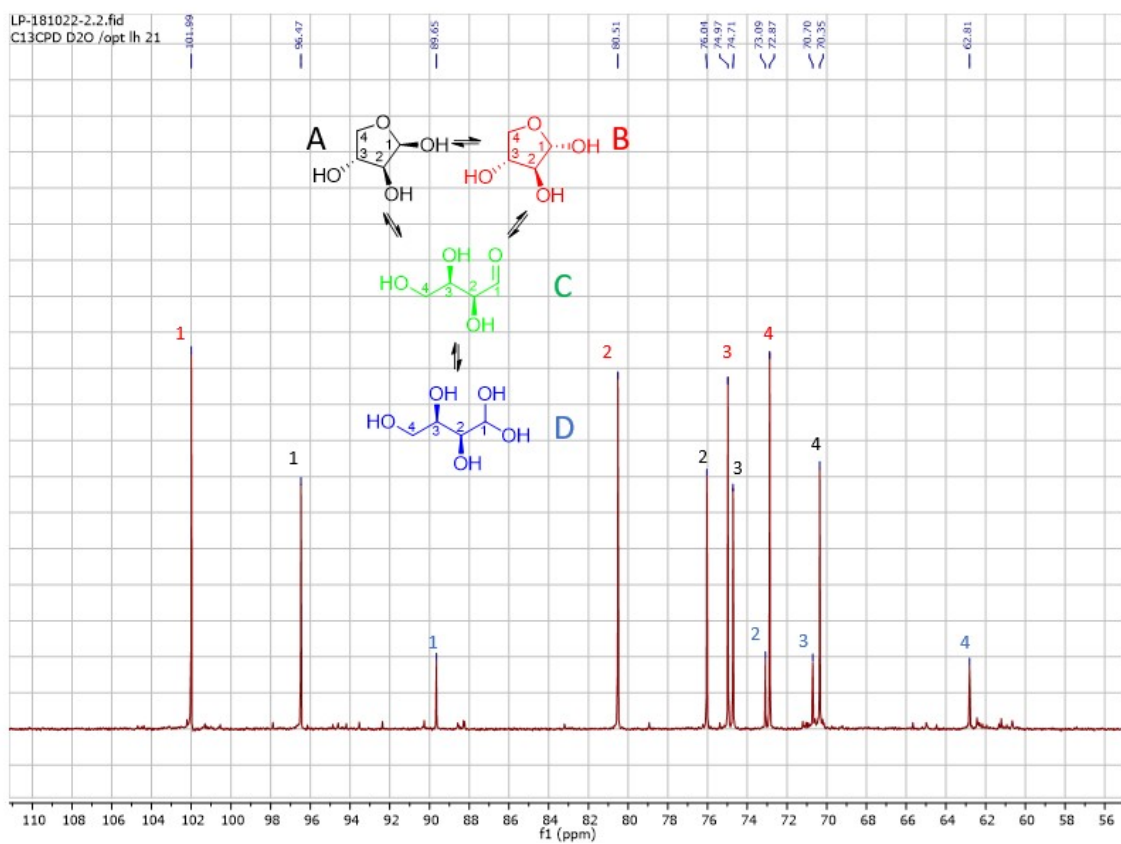


Figure S42 :  $^{13}\text{C}$  NMR spectrum of D-threose obtained with FSA<sub>AciBac</sub>

RMN  $^{13}\text{C}$  (100 MHz,  $\text{D}_2\text{O}$ )  $\delta$  102.0 ( $\text{C}^{\text{B}1}$ ), 96.5 ( $\text{C}^{\text{A}1}$ ), 89.7 ( $\text{C}^{\text{D}1}$ ), 80.5 ( $\text{C}^{\text{B}2}$ ), 76.0 ( $\text{C}^{\text{A}2}$ ), 75.0 ( $\text{C}^{\text{B}3}$ ), 74.7 ( $\text{C}^{\text{A}3}$ ), 73.1 ( $\text{C}^{\text{D}2}$ ), 72.9 ( $\text{C}^{\text{B}4}$ ), 70.7 ( $\text{C}^{\text{D}3}$ ), 70.4 ( $\text{C}^{\text{A}4}$ ), 62.8 ( $\text{C}^{\text{D}4}$ ).

#### 5.2. 2-deoxy-D-ribose-5-phosphate from acetaldehyde + D-glyceraldehyde-3-phosphate

In a flask were placed 600  $\mu\text{L}$  of an acetaldehyde solution (1 M, final 100 mM), 465  $\mu\text{L}$  of a DHAP solution (final 25 mM) and 5.1 mL of water. The pH of the solution was then adjusted to 7.5 and 100  $\mu\text{L}$  were taken to provide a blank. 25 mg of  $\text{FSA}_{\text{AciBac}}$  and 30  $\mu\text{L}$  of TPI (545 U) were then added. After 2 h of reaction at room temperature, 12 mg of  $\text{FSA}_{\text{AciBac}}$  and 200  $\mu\text{L}$  of acetaldehyde solution (1 M) were added. After additional 4 h of reaction at room temperature, 10 mg of  $\text{FSA}_{\text{AciBac}}$  enzyme and 200  $\mu\text{L}$  of acetaldehyde solution (1 M) were added. After 6h and 23 h of reaction, 200  $\mu\text{L}$  of acetaldehyde solution (1 M) was added to prevent acetaldehyde evaporation. An 84% disappearance of DHAP was achieved in 26 h. Then, the enzyme was discarded by IMAC technique and the solution lyophilized at pH 7.5. The solid was then washed with acetone, recovered by centrifugation and washed with ethanol. The solid was then taken up in water, passed through an ultra-centrifugal filter (Amicon<sup>TM</sup>) and lyophilized again. 85 mg of product was obtained. To accurately determine the amount of deoxyribose-5-phosphate, the solid was taken up in 1 mL of water and the deoxyribose-5-phosphate content determined using deoxyribose-5-phosphate aldolase (DERA) by UV-visible spectroscopy. 77  $\mu\text{mol}$  of product were found, corresponding to a 50% yield.

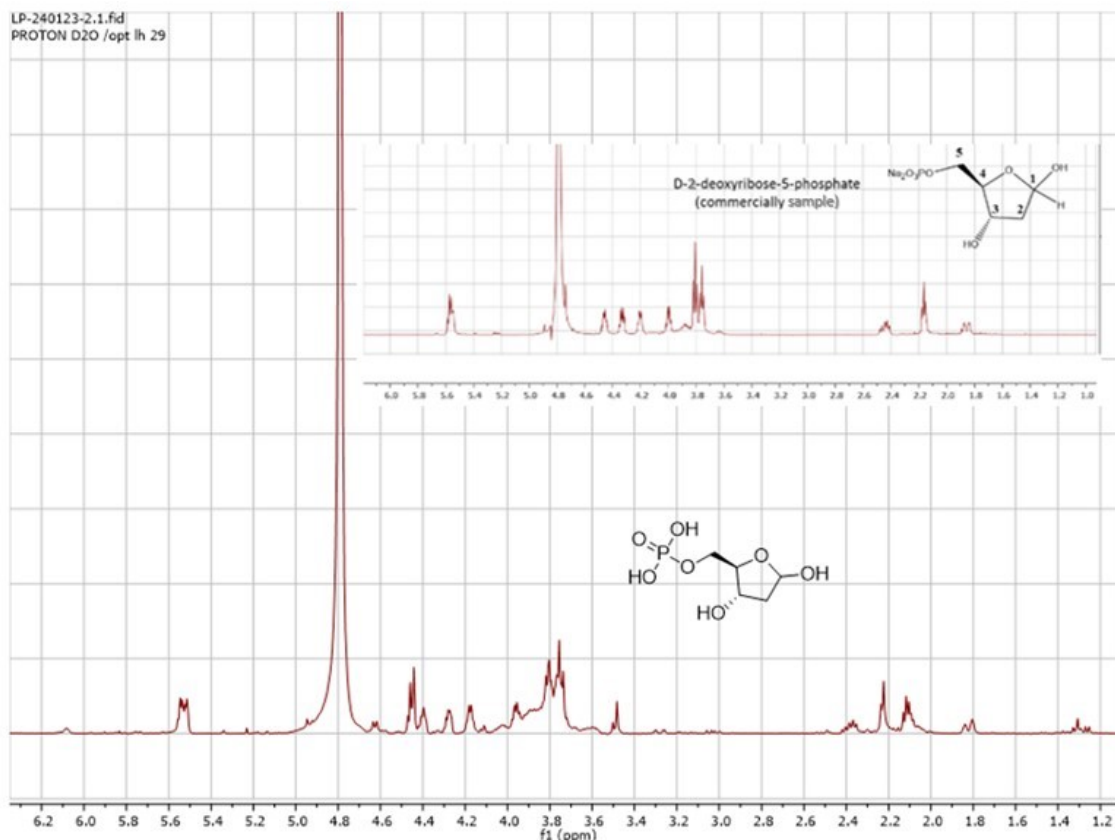


Figure S43 :  $^1\text{H}$  NMR of deoxyribose-5-phosphate obtained

5.3. (3*S*,4*S*) 5-chloro-3,4-dihydroxypentan-2-one from HA + chloroacetaldehyde

30  $\mu\text{L}$  (0.26 mmol) of a 55% chloroacetaldehyde solution in water, 26  $\mu\text{L}$  of HA (0.31 mmol) and 2.5 mL of water were placed in a flask. The pH of the solution was adjusted to 8.2 and 100  $\mu\text{L}$  was taken as a blank. 361  $\mu\text{L}$  of a FSA<sub>AcAeo</sub> solution (in ammonium sulphate 29 mg/mL) was centrifuged, the ammonium sulphate solid removed, and the supernatant containing the enzyme was added (final enzyme concentration: 4 mg/mL). After 12 h of reaction, the protein was removed on an ultra-centrifugal filter (Amicon<sup>TM</sup>) and the mixture evaporated at reduced pressure. 52.9 mg of product were obtained as a white/translucent solid. Since the compound tended to sublime easily, to determine the salts quantity, the compound was totally sublimated by lyophilization leading to 19.4 mg of salts thus corresponding to an 85% yield (33.5 mg).

RMN  $^1\text{H}$  (400 MHz, D<sub>2</sub>O)  $\delta$  4,54 (d,  $J = 2.0$  Hz, 1H, H<sup>3</sup>), 4,38 (m, 1H, H<sup>4</sup>), 3,71 (m, 2H, H<sup>5</sup>, H<sup>5'</sup>), 2,31 (s, 3H, H<sup>1</sup>).

RMN  $^{13}\text{C}$  (100 MHz, D<sub>2</sub>O)  $\delta$  212.5 (C<sup>2</sup>), 77.0 (C<sup>3</sup>), 71.4 (C<sup>4</sup>), 44.5 (C<sup>5</sup>), 25.7 (C<sup>1</sup>).

HRMS ESI-:  $m/z$  calcd. for  $[\text{C}_5\text{H}_9\text{ClO}_3, \text{HCO}_2]^- = 197.0222$ ; found 197.0210.

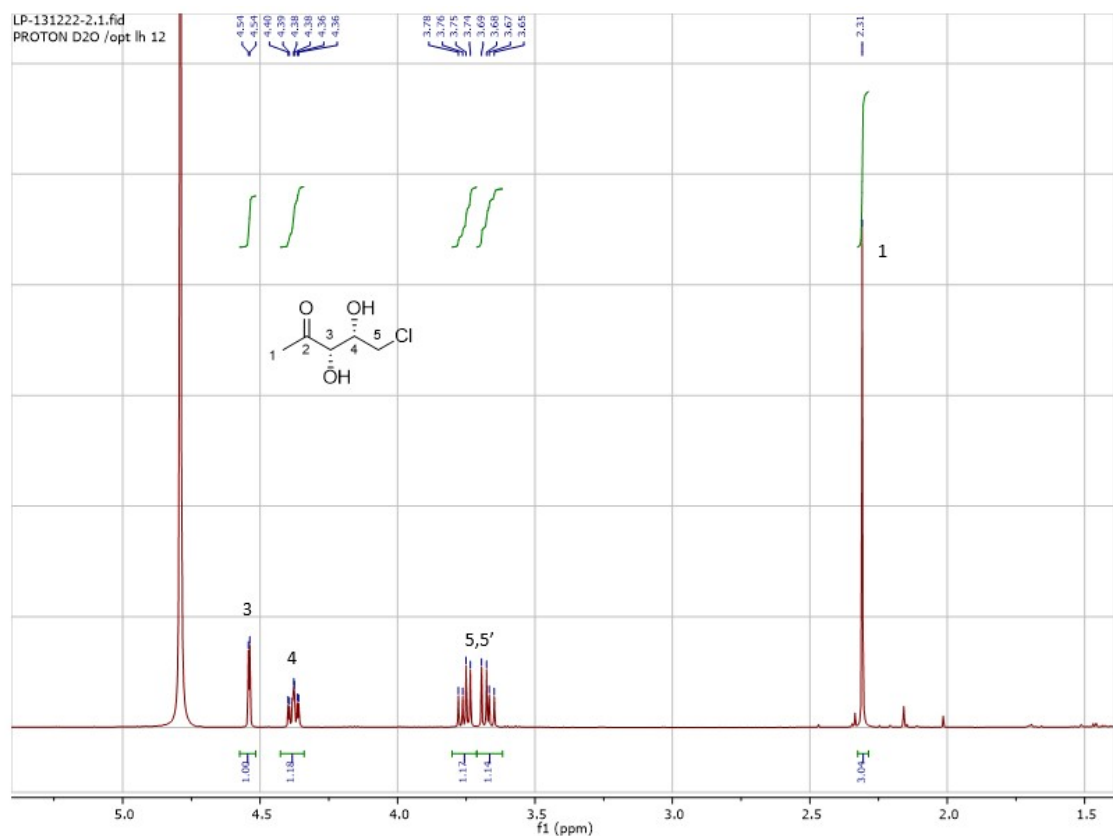


Figure S44 :  $^1\text{H}$  NMR of the product obtained by coupling HA+chloroacetaldehyde with FSA<sub>AcAeo</sub>

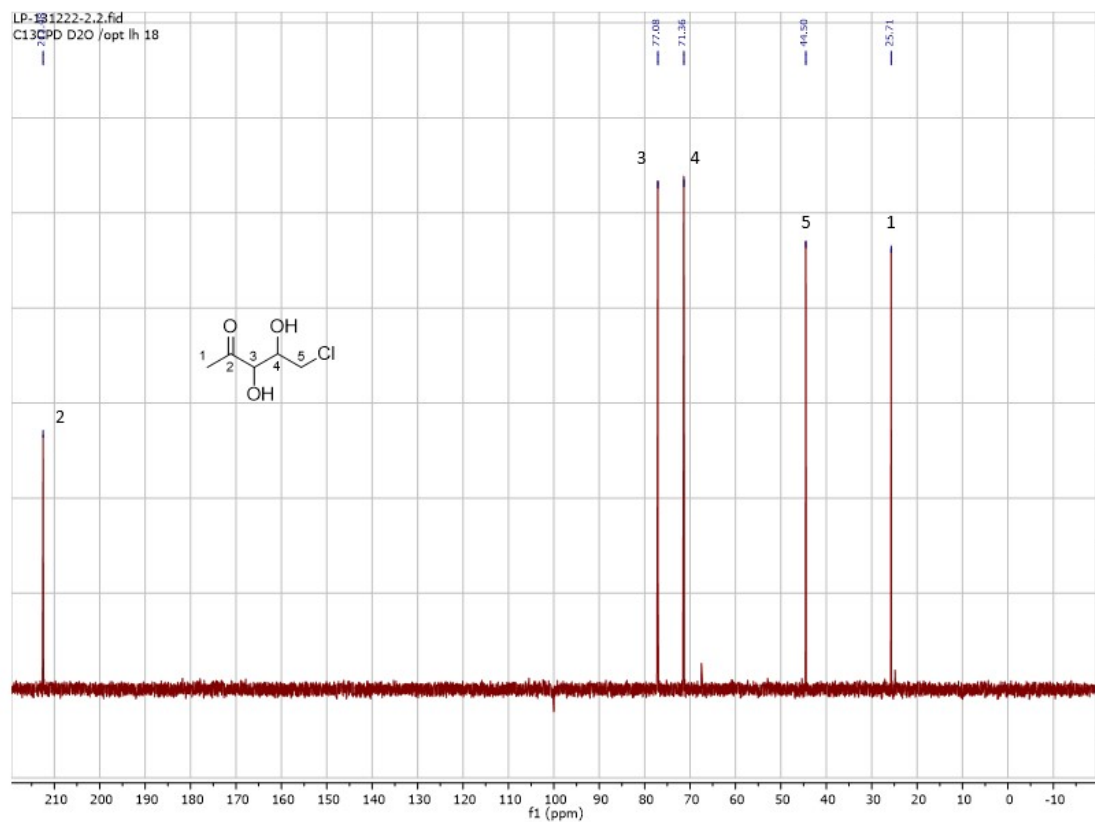


Figure S45 :  $^{13}\text{C}$  NMR of the product obtained by coupling HA+chloroacetaldehyde with FSA<sub>AcAeo</sub>

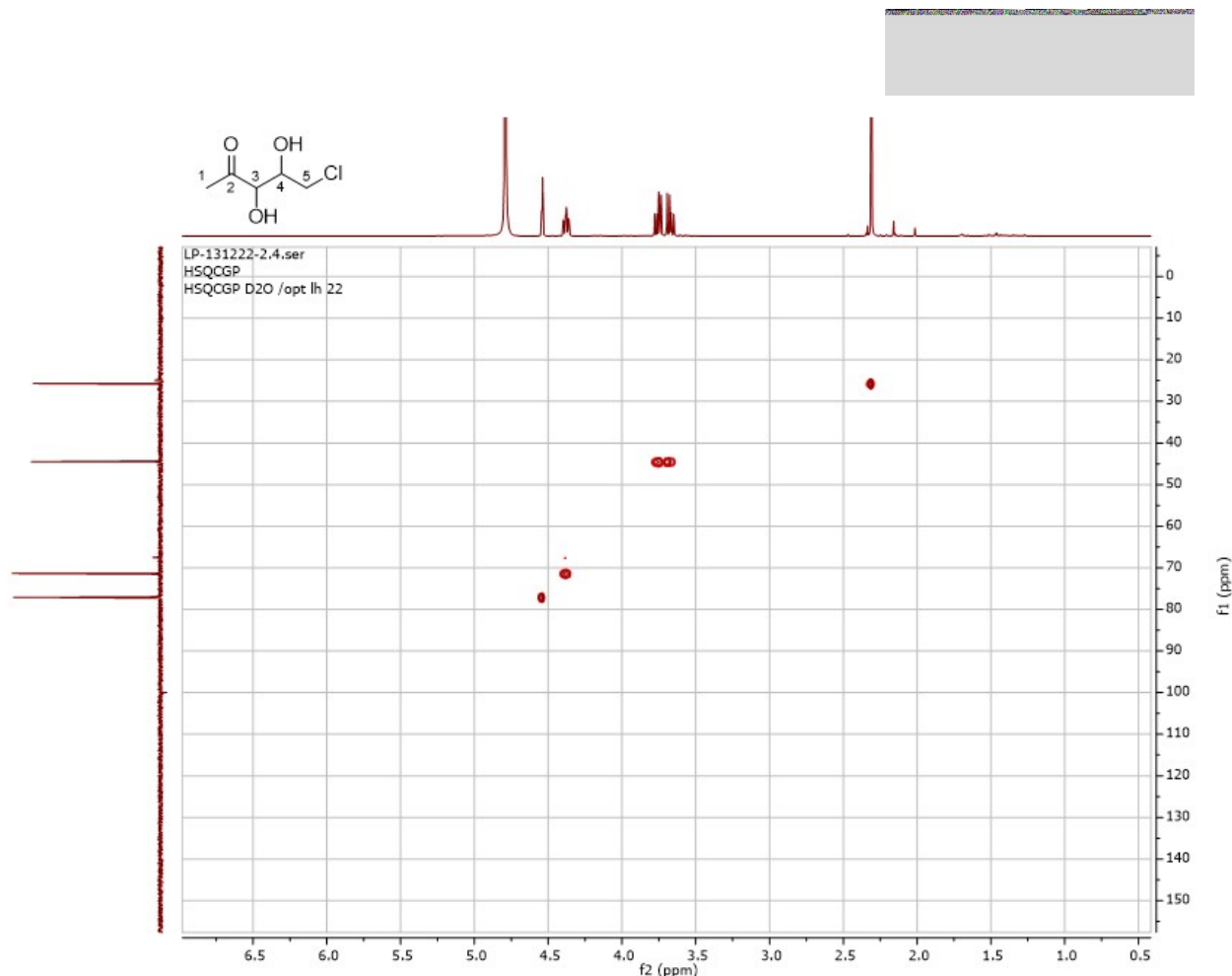


Figure S46 : HSQC of the product obtained by coupling HA+chloroacetaldehyde with FSA<sub>AcAeo</sub>

#### 5.4. (3S,4S) 3,4-dihydroxypentanal from acetaldehyde + L-lactaldehyde

A flask was filled with 4.5 mL of a solution of L-lactaldehyde (93 mM, final 50 mM), 485  $\mu$ L of an acetaldehyde solution (1.75 M, final 100 mM) and 3.4 mL of water. The pH was then adjusted to 7.9 and 100  $\mu$ L were collected for a blank. 1.4 g of cells were added after being washed 3 times with water to remove the glycerol added for conservation. After 48 h, the mixture was centrifuged at 8000 rpm for 20 min and the supernatant collected. The cells were washed with 2x15 mL of water and the mixture centrifuged. The supernatants were combined and evaporated *in vacuo*. Purification was performed on a silica gel column (eluent: AcOEt). 30.9 mg of product were obtained (62% yield).

RMN <sup>1</sup>H (400 MHz, D<sub>2</sub>O)  $\delta$  5.57 (t,  $J$  = 4.7 Hz, 1H, H<sup>1</sup>), 4,25 (m, 1H, H<sup>3</sup>), 4.21-4.14 (m, 1H, H<sup>4</sup>), 2.15 (m, 2H, H<sup>2</sup>, H<sup>2'</sup>), 1.16 (d, 3H, H<sup>5</sup>).

RMN <sup>13</sup>C (major form) (100 MHz, D<sub>2</sub>O)  $\delta$  96.8 (C<sup>1</sup>), 77.5 (C<sup>4</sup>), 72.5 (C<sup>3</sup>), 42.4 (C<sup>2</sup>), 12.9 (C<sup>5</sup>).

RMN <sup>13</sup>C (minor form) (100 MHz, D<sub>2</sub>O)  $\delta$  97.2 (C<sup>1</sup>), 79.3 (C<sup>4</sup>), 71.0 (C<sup>3</sup>), 41.2 (C<sup>2</sup>), 14.1 (C<sup>5</sup>).

HRMS ESI-: m/z calcd. for [C<sub>5</sub>H<sub>10</sub>O<sub>3</sub>, HCO<sub>2</sub>]<sup>-</sup> = 163.0612; found 163.0600.



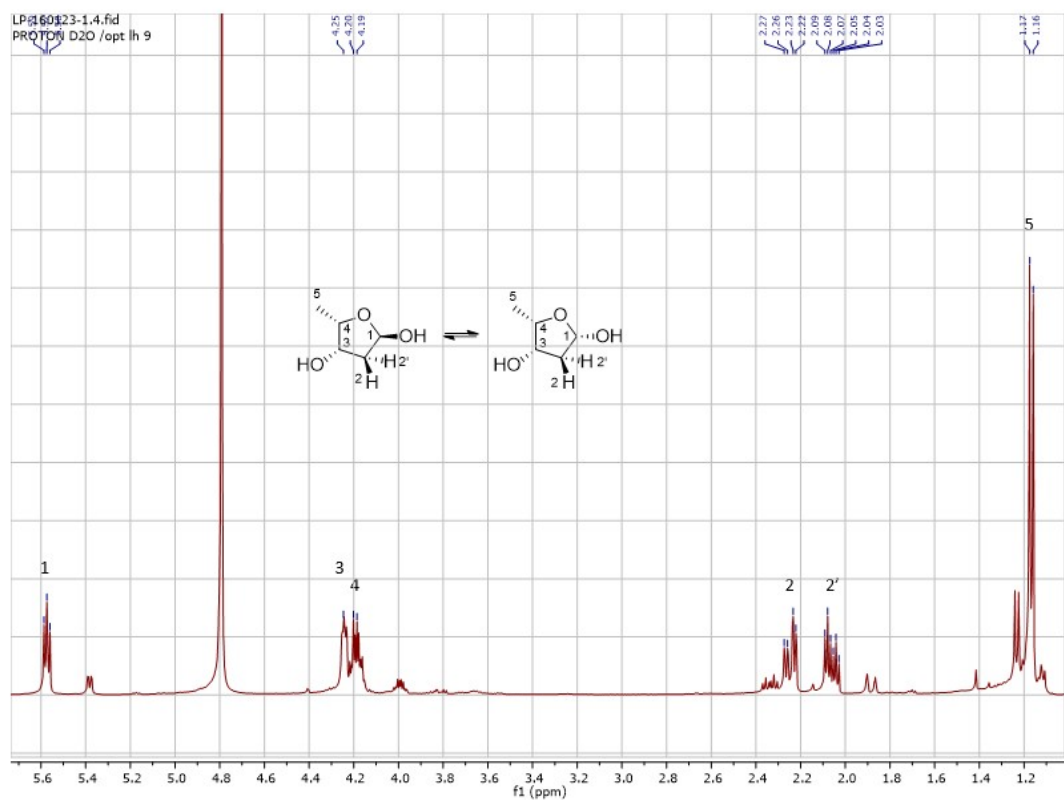


Figure S47 :  $^1\text{H}$  NMR of the product obtained by coupling acetaldehyde+L-lactaldehyde with  $\text{FSA}_{\text{AcAeo}}$

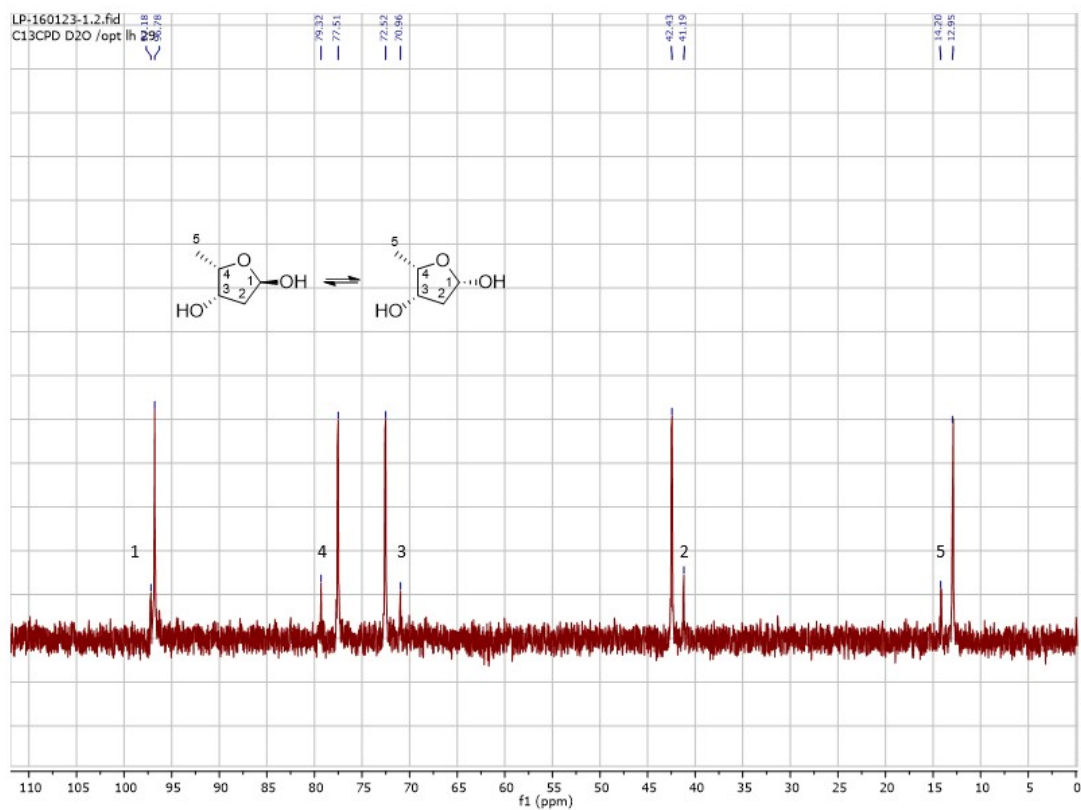


Figure S48 :  $^{13}\text{C}$  NMR of the product obtained by coupling acetaldehyde+L-lactaldehyde with  $\text{FSA}_{\text{AcAeo}}$

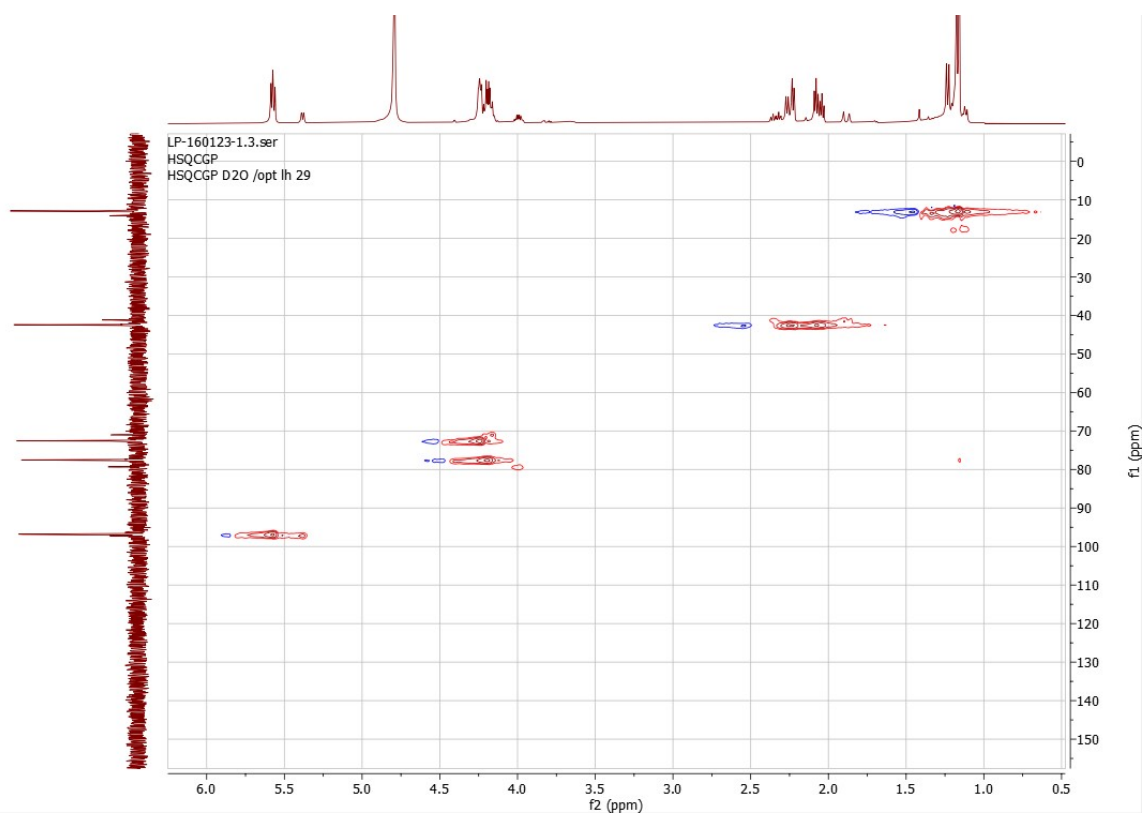


Figure S49 : HSQC of the product obtained by coupling acetaldehyde+L-lactaldehyde with  $\text{FSA}_{\text{AcAeo}}$

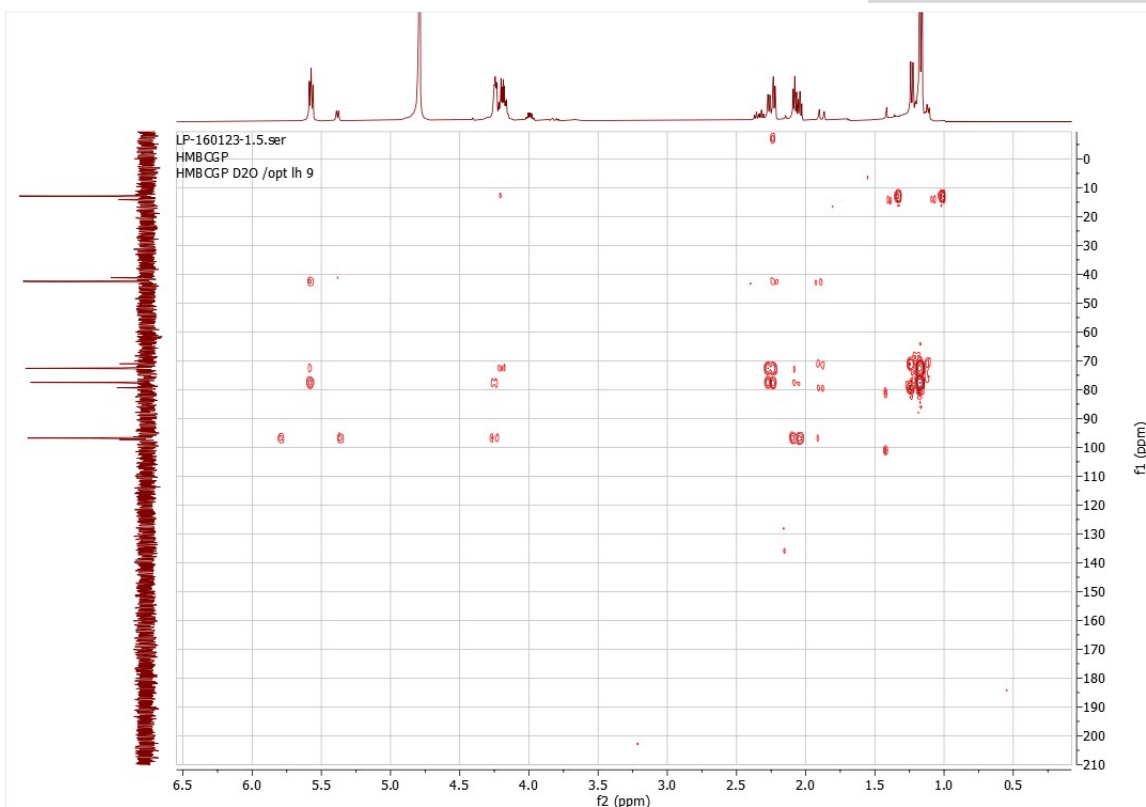



Figure S50 : HMBC of the product obtained by coupling acetaldehyde+L-lactaldehyde with FSA<sub>AcAeo</sub>

## References

- (1) Schneider, S.; Gutiérrez, M.; Sandalova, T.; Schneider, G.; Clapés, P.; Sprenger, G. A.; Samland, A. K. Redesigning the Active Site of Transaldolase TalB from Escherichia Coli: New Variants with Improved Affinity towards Nonphosphorylated Substrates. *ChemBioChem* **2010**, *11* (5), 681–690. <https://doi.org/10.1002/cbic.200900720>.
- (2) Vergne-Vaxelaire, C.; Bordier, F.; Fossey, A.; Besnard-Gonnet, M.; Debard, A.; Mariage, A.; Pellouin, V.; Perret, A.; Petit, J.-L.; Stam, M.; Salanoubat, M.; Weissenbach, J.; De Berardinis, V.; Zapparucha, A. Nitrilase Activity Screening on Structurally Diverse Substrates: Providing Biocatalytic Tools for Organic Synthesis. *Adv. Synth. Catal.* **2013**, *355* (9), 1763–1779. <https://doi.org/10.1002/adsc.201201098>.
- (3) Paulat, L.; Laurent, V.; Hélaïne, V.; Théveniot, M.; Petit, J.; Lemaire, M.; Delmas, V.; Bouzon, M.; De Berardinis, V.; Guérard-Hélaïne, C. Insights on DHAP Aldolases Ability to Convert Dioxxygen or a Ketone as Electrophile: Use of a Strain Depleted in Triose Phosphate Isomerase. *ChemCatChem* **2024**, e202400202. <https://doi.org/10.1002/cctc.202400202>.
- (4) Thorell, S.; Schürmann, M.; Sprenger, G. A.; Schneider, G. Crystal Structure of Decameric Fructose-6-Phosphate Aldolase from Escherichia Coli Reveals Inter-Subunit Helix Swapping as a Structural Basis for Assembly Differences in the Transaldolase Family. *J. Mol. Biol.* **2002**, *319* (1), 161–171. [https://doi.org/10.1016/S0022-2836\(02\)00258-9](https://doi.org/10.1016/S0022-2836(02)00258-9).
- (5) Lehweß-Litzmann, A.; Neumann, P.; Parthier, C.; Lütke, S.; Golbik, R.; Ficner, R.; Tittmann, K. Twisted Schiff Base Intermediates and Substrate Locale Revise Transaldolase Mechanism. *Nat. Chem. Biol.* **2011**, *7* (10), 678–684. <https://doi.org/10.1038/nchembio.633>.

- 
- (6) Samland, A. K.; Baier, S.; Schürmann, M.; Inoue, T.; Huf, S.; Schneider, G.; Sprenger, G. A.; Sandalova, T. Conservation of Structure and Mechanism within the Transaldolase Enzyme Family. *FEBS J.* **2012**, *279* (5), 766–778. <https://doi.org/10.1111/j.1742-4658.2011.08467.x>.
- (7) Stellmacher, L.; Sandalova, T.; Leptihn, S.; Schneider, G.; Sprenger, G. A.; Samland, A. K. Acid-Base Catalyst Discriminates between a Fructose 6-Phosphate Aldolase and a Transaldolase. *ChemCatChem* **2015**, *7* (19), 3140–3151. <https://doi.org/10.1002/cctc.201500478>.
- (8) Sautner, V.; Friedrich, M. M.; Lehwess-Litzmann, A.; Tittmann, K. Converting Transaldolase into Aldolase through Swapping of the Multifunctional Acid–Base Catalyst: Common and Divergent Catalytic Principles in F6P Aldolase and Transaldolase. *Biochemistry* **2015**, *54* (29), 4475–4486. <https://doi.org/10.1021/acs.biochem.5b00283>.
- (9) Yang, X.; Wu, L.; Li, A.; Ye, L.; Zhou, J.; Yu, H. The Engineering of Decameric D -Fructose-6-Phosphate Aldolase A by Combinatorial Modulation of Inter- and Intra-Subunit Interactions. *Chem. Commun.* **2020**, *56* (55), 7561–7564. <https://doi.org/10.1039/D0CC02437F>.
- (10) Webb, B.; Sali, A. Comparative Protein Structure Modeling Using MODELLER. *Curr. Protoc. Bioinforma.* **2016**, *54* (1). <https://doi.org/10.1002/cpbi.3>.
- (11) Pettersen, E. F.; Goddard, T. D.; Huang, C. C.; Couch, G. S.; Greenblatt, D. M.; Meng, E. C.; Ferrin, T. E. UCSF Chimera?A Visualization System for Exploratory Research and Analysis. *J. Comput. Chem.* **2004**, *25* (13), 1605–1612. <https://doi.org/10.1002/jcc.20084>.
- (12) Varadi, M.; Anyango, S.; Deshpande, M.; Nair, S.; Natassia, C.; Yordanova, G.; Yuan, D.; Stroe, O.; Wood, G.; Laydon, A.; Žídek, A.; Green, T.; Tunyasuvunakool, K.; Petersen, S.; Jumper, J.; Clancy, E.; Green, R.; Vora, A.; Lutfi, M.; Figurnov, M.; Cowie, A.; Hobbs, N.; Kohli, P.; Kleywegt, G.; Birney, E.; Hassabis, D.; Velankar, S. AlphaFold Protein Structure Database: Massively Expanding the Structural Coverage of Protein-Sequence Space with High-Accuracy Models. *Nucleic Acids Res.* **2022**, *50* (D1), D439–D444. <https://doi.org/10.1093/nar/gkab1061>.
- (13) Morris, G. M.; Huey, R.; Lindstrom, W.; Sanner, M. F.; Belew, R. K.; Goodsell, D. S.; Olson, A. J. AutoDock4 and AutoDockTools4: Automated Docking with Selective Receptor Flexibility. *J. Comput. Chem.* **2009**, *30* (16), 2785–2791. <https://doi.org/10.1002/jcc.21256>.
-